LATE PLEISTOCENE TO MIDDLE HOLOCENE PALEOLIMNOLOGICAL VARIABILITY PRESERVED IN THE SEDIMENTS OF WALDEN POND, MA.

Honors Thesis

Presented in Partial Fulfillment of the Requirements

For the Degree of Bachelor of Science

In the Department of Geological Sciences

at Salem State University

By

Hannah Newcombe

Dr. J. Bradford Hubeny
Faculty Advisor
Department of Geological Sciences

***

Commonwealth Honors Program

Salem State University

2019

Abstract

After the Last Glacial Maximum, the climate of the Northern Hemisphere exhibited a general warming pattern until a period of time recognized as the Holocene Climatic Optimum. The trend of gradual warming was disrupted by multiple climatic events. Of these events, the most notable is the Younger Dryas. This is the cooling event that defines the end of the Pleistocene Epoch. The purpose of this study is to reconstruct paleolimnological environmental conditions in Eastern Massachusetts during the period of time bracketed by the Younger Dryas (YD) and the Holocene Climatic Optimum (HCO) and to test the hypothesis that these changes are sensitive to regional climate change. We utilized the sediment archival record preserved in Walden Pond (Concord, MA) for this study, specifically the proxy records of stable carbon, nitrogen, and sulfur isotopes. Initial sub-bottom SONAR data taken in 2016 indicated a thick sediment package in the deep western basin of the pond, and in 2017 a Livingstone sediment core recovered approximately 9 meters of sediment. Eleven AMS radiocarbon dates were used to calculate an age model of the core, and the model calculates a basal age of 13,775 $\pm$ 280 cal BP. Sediment samples taken at 2 cm intervals down the depth of the core reveal a relatively low %OC at the base of the core. This value is about 5.00% and starts drastically increasing to high of 18.00% OC at age 11,671 BP. This trend in increasing %OC matches with a display of an increasing sedimentation rate which occurs as we pull out of the Younger Dryas. With an increasing sedimentation rate and an increasing %OC, it becomes evident that there is an increase in productivity within water column. When comparing the sedimentation rate and the %OC to the δ13Cvalues become less depleted ranging from -28.00‰ to -23.00‰ between the base of the core up to 4000 yrs. BP with some fluxes in between. Increased productivity and poor mixing are both contributors to increased δ13C. Walden Pond is a contained environment with no input of water from rivers or streams. The main sediment source is surrounding matter, windblown sediment and precipitation. The Younger Dryas displays an evident signature in the data with abrupt changes in sedimentation rates and low percentages of organic carbon. Coming out of the cold, arid conditions of the YD and into relatively warmer temperatures, increased productivity and influx of organic matter can be expected. δ15N can also indicate rates of productivity, although the current data shows a stable curve with values remaining between 2.00‰ and 4.00‰.

Acknowledgments

This study could not have been done without the help of my advisor, Brad Hubeny. Thank you so much for introducing me to this project and allowing me to contribute research to the science world. This research could also not have been done without the help of Renee Knudstrup. Thank you for all your help in and out of the lab, I could not have completed this work without you. In addition, I would like to thank Honors Program Chair, Scott Nowka for helping me along the way. An extended thanks goes out to the entire Geology Faculty, thank you for your feedback and support. I would also like to acknowledge my colleagues and a special thanks to Danielle Hartford for standing with me two hours while I presented my research at NEGSA. Lastly, I would like to thank my friends, family and boyfriend for all your support.

Table of Contents

List of Figures

intermittent oxidized material. Three distinct centimeter thick bands are shown in the zoom in on the figure at 765 cm, 768 cm and 829 cm.

Figure 15 - Scree plot with broken stick (red). This plot shows the significance of PC1 and PC2 as they plot above the red line. This shows each component vs the % eigenvalue.

Figure 16 - PC1 loadings vs depth centimeters downcore plot. Values greater than zero can be interpreted as increased productivity where values less than zero can be interpreted as decreased productivity. Green is HCO, red is 8.2 Kiloyear and blue is YD.

Figure 17 - PC2 downcore plot vs depth in centimeters. Values less than zero can be interpreted as more oxidation - reduction and values greater than zero can be interpreted as less oxidation - reduction. Green is HCO, red is 8.2 Kiloyear and blue is YD.

Figure 18 - Spectral analysis of $\delta^{13}C$. Periodicity is labelled at 99%, 95% and 90% confidence intervals. Cycles are observed at 275, 170 and 93 years.

Figure 19 - Organic carbon percentage spectral analysis. Periodicity is labelled at 99%, 95% and 90% confidence levels. Cycles are observed at 460, 266, 224 and 160 years.

Figure 20 - $\delta^{15}N$ spectral analysis. Periodicity is labelled at 99% confidence levels. Cycles are observed at 313, 195 and 103 years.

Figure 21- Percent nitrogen spectral analysis. Periodicity is labelled at 99%, 95% and 90% confidence levels. Cycles are observed at 221, 143, 125, 106 and 99 years.

Figure 22- Organic carbon to nitrogen ratio spectral analysis. Periodicity is labelled at 95% and 90% confidence levels. Cycles are observed at 444, 276, 138, 122 and 115 years.

Figure 23 - $\delta^{34}S$ spectral analysis. Periodicity is labelled at 90% confidence levels. Cycles are observed at 140, 125 and 113 years.

Figure 24 - Sulfur percentage spectral analysis. Periodicity is labelled at 95% and 90% confidence levels. Cycles are observed at 146, 125 and 100 years.

Figure 25 - Organic carbon to sulfur ratio spectral analysis. Periodicity is labelled at 99% and 95% confidence levels. Cycles are observed at 127, 118 and 114 years.

Figure 26 - Principal component 1 spectral analysis. Periodicity is labelled at 99% and 95% confidence levels. Cycles are observed at 232, 205 and 145 years.

Figure 27- Principal component 2 spectral analysis. Periodicity is labelled at 99%, 95% and 90% confidence levels. Cycles are observed at 468, 267, 226, 153, 120 and 113 years.

List of Tables

1. Introduction

Lake sediments can be used to tell the story of climate change. Since the Last Glacial Maximum (LGM), climate on earth has changed significantly. A culmination of different records has documented climatic events in the northern hemisphere. Of these events, two well-known are the Younger Dryas (YD) and the Mid Holocene Climatic Optimum (HCO).

This study is focusing on how a lacustrine environment responds to the climatic changes coming out of the cold, dry YD and into the warm, wet HCO. Walden Pond located in Eastern Massachusetts (Figure 1) is the field area being studied for this research to interpret paleoclimates and the paleoenvironment associated with Northern Hemispheric climatic oscillation patterns. Using a multiproxy isotopic analysis, this study will test the hypothesis that Walden Pond is sensitive to regional and hemispheric climate change bracketed by the Younger Dryas and the Mid Holocene Climatic Optimum. With the past environment as a frame of reference, one goal will be to identify changes in the climate and if well documented paleo events, such as the 8.2 Kiloyear event, are identified this study will attempt to understand what forcing attribute to these climatic shifts.

1.1 Field Area

Walden Pond, made famous by Henry David Thoreau, is home to Massachusetts' deepest lake. The lake is a textbook kettle hole created from chunks of ice left behind during the Last Glacial Maximum (Coleman and Friesz, 2001) which ended approximately 15,000 years ago. Walden Pond became an area of interest after studies of the recent past (last 1,600 years) showed substantial isotopic data including changes in nutrients (Koster et al, 2005). Brad Hubeny and colleagues have studied paleoclimate at other lakes in the New England Region (Hubeny et al., 2015) and wanted to add this lake to their cumulative records. The lake is a closed system with no input or output of water. The residence time is approximately 5 years (Coleman and Friesz, 2001). There are three deep basins within the lake, the deepest being 30.5 m as originally observed by Henry David Thoreau. Underneath the fine-grained sediment is primarily till and glacial outwash. The bedrock is granite (Koteff, 1964). Preliminary field work (Knights et al. 2017), including sub bottom bathymetry, revealed four deep basins within the lake. Based on this information, a location

for a Livingstone long core was determined (Figure 1). Taking a core from the deepest basin (Figure 2) will provide the best continuous core record. This core will be used to obtain the data for this study.

1.2 Younger Dryas

Ice sheets in the Northern Hemisphere reached their maximum extent around 26,500 years ago (cal BP) (Clark et al. 2009). This climatic event is known as the Last Glacial Maximum (LGM). Around 20,000 years ago (cal BP), the increase of northern summer insolation allowed for deglaciation to begin and temperatures to increase (Clark et al. 2009). The gradual warming after the LGM, however, was abruptly reversed by a cooling event that mimicked the LGM on a much smaller scaled. The Younger Dryas is named after the plant, *Dryas octopetala,* which grows in cold conditions. The YD is a well-documented climatic cooling. Greenland ice core GICC05 chronology estimates the interval to be 12,900-11,700 years BP (Rasmussen et al., 2006; Thomas et al., 2007). A wetland sediment core from New York estimates the YD to occur between 12,600-11,600 years BP (Kirby et al. 2002; Alley et al. 1993). For the purposes of this research, the YD will be defined as occurring between 13,000 to 11,500 years BP based on the culmination of records.

The Younger Dryas is the best studied 'millennial-scale cold snap of glacial time' (Broecker et. al 2009). Its origin is debated but recent evidence shows that this cold period is a significant part of the deglaciation sequence (Broecker et al. 2009). Evidence for the YD is visible in many parts of the world, but the strongest and most abundant evidence is found in the Northern Hemisphere (Alley 2000; Brauer et al. 2008). New England temperatures were decreased by 7.5 degrees Celsius (Dorale et al. 2010). With abrupt changes in climate and decreasing temperature, the Younger Dryas significantly impacted vegetation and other environmental aspects. The Younger Dryas is defined as a chronozone (Mangerud et. al 1974) because the vegetational and climatic events that appear in different records can only be correlated through $\delta^{14}C$ chronology (Peteet 1995). Conditions during the Younger Dryas were not only cooler in temperature but also dry and arid (Dorale et al. 2010). During the YD, concentrations of pollen in the sediment are minimal (Brauer et al. 1999). Preliminary pollen analysis from Walden Pond show during the defined interval,

increased pine and softwood pollen grains (Figure 3). This data helps to constrain the ages and evidence of YD before isotopic proxies are run and age dates are obtained.

1.3 Mid Holocene Climatic Optimum

The Mid Holocene Climatic Optimum or hypsithermal is a period of geological time that occurred in recent past that was warmer than present day. The interval of this event ranges from 9,000 to 5,000 years ago BP. For the purpose of this study, the interval of the HCO will be defined as 7,000 to 5,000 years BP (Bartlein et al. 2011; NOAA). Ice core delta records from West Antarctica and Northwest Greenland were compared (GRIP and NGRIP) and both show post glacial climatic optimum (Dansgaard 2004). During this event in the middle of the Holocene, summer temperatures in the Northern Hemisphere were warmer than today (Davis et al. 2003). The Intergovernmental Panel on Climate Change's Fifth Assessment Report illustrates the mean temperature anomaly is between 2-5℃ during the warmest month. This climatic event is most likely associated with Milankovitch cycles or predictable changes in Earth's orbit. The effect of this cycle relates to maximum Northern Hemispheric heating and the nearest approach to the sun. Around this time, the tilt of Earth's axis was about 24 degrees (Ruddiman 2014)

Changes in the temperature also caused for weather changes. Reports include significantly wetter conditions. During the defined interval, Walden Pond's pollen record shows increase oak and hardwood pollen grains. This type of vegetation prefers more moderate temperatures (Figure 3).

1.4 The 8.2 Kiloyear Event

In between the Mid Holocene Climatic Optimum and the Younger Dryas, evidence for a smaller scale climatic event has been recorded in research. Although the focus of this research is on the potential impact of the HCO and the YD, it is important to note if the 8.2 Kiloyear Event can be observed within this record. The 8.2 Kiloyear Event was a sudden drop in temperature after the warming of the YD by 1-3℃ (Matero et al. 2017). This event occurred approximately 8,200 years BP and was first identified by Heinrich Zollar. Strongest evidence for this event is located in the Northern Hemisphere and found in

Greenland ice cores and other records and is most notable for changes in sea-level. A culmination of research concluded that early in the Holocene, glacial lakes including Lake Agassiz drained into the Hudson Bay. This moved downstream to the Labrador Sea ultimately slowing deep-water formation and thermohaline circulation (Ellison et. al, 2006). This event may replicate the effects of the YD but, having only lasted approximately 200 years, response times and feedback may not be evident. For the purpose of this study, the 8.2 kiloyear event will be defined by the interval 8,200 to 8,000 years BP (Matero et al. 2017; Kirby et al. 2002).

1.5 Organic Matter

Organic matter is a proxy that is frequently used when studying lake sediment records. This is because it holds sensitivity to past environments and holds relative post-depositional stability. Organic matter can be used from lakes to help interpret what the environment may have looked like in the past. This field of study is known as paleolimnology. According to Meyer (1997), organic matter can be defined as a mix of lipids, carbohydrates, proteins and other organic materials. In lake sediments we may find evidence of vegetation, or geochemical fossils that can be used for interpretation. Organic matter can help us study both natural and human induced changes that may have taken place in lacustrine system. The paleolimnological proxies for lake sediments show plants being the primary source of organic matter. Plants can be divided into two geochemically distinct groups. There are non-vascular plants with little to no carbon rich cellulose or lignin. The other kind of plants are vascular plants that contain large proportions of fibrous tissue. When studying organic matter in lake sediment, we can find both the type and amount of matter the extent of alteration and degradation is occurring within the sediment.

1.6 Stable Isotopes

In order to interpret these climatic events at Walden Pond, three stable isotopes and their elemental concentrations will be utilized. These are carbon, nitrogen and sulfur. Productivity has geochemical processes which can be studied through carbon and nitrogen, this will allow part of the paleoclimate reconstruction (Bertrand et al., 2010; Meyers and Ishiwatari, 1993). These proxies will also be useful when understanding photosynthesis

and source of organic matter within the lake (Meyers and Ishiwatari, 1993). Sulfur variability in late sediments can represent shifts in reducing and producing sulfate conditions as well as mixing in the water column consistent with hypoxic and anoxic conditions (Aizenshtat and Amrani, 2004; Rudd et al., 1986).

1.6.1 Carbon

In organic matter, the ratio of $\delta^{13}C$ can be interpreted in a few ways. The most likely interpretations for this study are productivity, nutrient availability and organic matter sources (Meyers and Terranes 2001). Plants that are photosynthesized through C_3 have a $\delta^{13}C$ composition between -22.00‰ and -33.00‰ where plants that photosynthesize through C_4 have a heavier $\delta^{13}C$ composition ranging between -8.00‰ to -22.00‰ (Meyers and Terranes 2001). The C_3 plants optimal conditions are warmer and wetter climates whereas C_4 plants prefer cool, arid climates with low lake levels (Huang et al., 2006; Meyers and Lallier-Verges, 1999).

1.6.2 Nitrogen

Isotopic nitrogen concentrations may relate to nutrient sources and plant type, non-vascular and vascular. Aquatic plants have dissolved nitrate with an isotopic concentration of 7.00‰ to 10.00‰ where $\delta^{15}N$ in terrestrial plants is generally 0.00‰ (Meyers and Lallier-Verges, 1999).

1.6.3 Carbon to Nitrogen Ratio

Organic carbon and nitrogen ratios (OC/N) in algae and vascular plants can determine whether the organic matter originated from land or aquatic sources. Phytoplankton have a 4-10 OC/N ratio where vascular land plants have 20> OC/N ratio (Meyers and Terannes 2001). Sometimes, OC/N ratios may give misleading indications of bulk organic matter. This leads to the interpretation that lakes that have a smaller amount of organic matter from vascular plants, relative to the water column production, have lower OC/N ratios in sediments than lakes that are accumulating large amounts of vascular plant debris. Partial degradation of organic matter during early diagenesis can modify elemental compositions. This will have an impact on the OC/N ratios of organic matter in sediment.

Most lakes have OC/N ratios of 13-14 which is indicative of a mix between the two sources (Meyers and Lallier-Verges, 1999).

2. Methods

2.1 Preliminary work

Walden Pond is an area of interest when studying paleoclimate because it the deepest lake in Massachusetts and extensive research has yet to be done on its sediment archive. Some work was done by Paul J. Friesz and John A. Colman in 2001 to understand Walden Pond's hydrology. Three deep basins are defined in the lake but the middle of the three has not been investigated up until 2001. It was determined that the deepest part of the lake was nearly 30.5 meters deep (Friesz and Colman, 2001). For the purpose of this study, a core was obtained from the deepest basin in Walden Pond because there was a sizable amount of sediment accumulation there. The sediment in Walden Pond ranges from fine to coarse grain sands that were deposited by glacial meltwater (Koteff, 1963). Additional sediment sources are near freshwater inputs. Sediment deposited in lake basins is affected by sediment focusing which distributes particles in deeper water thus having a greater amount of sediment accumulation in the deepest basin (Linkens and Davis, 1975). In 2015, previous geophysical work had been conducted by Brad Hubeny and Cooper Knights. Sub-bottom seismic reflection data was obtained using StrataBox HD hardware with SonarWiz software and a Garmin GPS unit. The data was then processed using SonarWiz5 at Salem State University. Seismic reflectors (bedrock or till) defined the basement of the lake and revealed the three basins of the lake. This data also revealed sediment accumulation in the basins (Figure 2) (Knights, 2017)

2.2 Field Work

After the area of interest within the lake was targeted, Brad Hubeny received permission to take the first ever long core from Walden Pond. In June 2017 a Livingstone core (WAL17_LC1) was extracted using a piston corer at location 0307436, 4701221 19T (z=29.6m).

2.3 Lab Work

Nine core sections were obtained and extruded into PVC liner, split lengthwise in the lab, and store at 4°C. An age-depth model was developed for the basin core using the program BACON. Two main age constraints were utilized, including, 11 calibrated AMS 14C dates and pollen data from the core (Figure 4). Half of the core was measured from top to bottom and marked at every centimeter to obtain samples. The other half is being preserved but was used to obtain six samples that were sent to the Woods Hole Oceanographic Institute (WHOI) for carbon dating. Samples (1 cm^3) were taken every centimeter from each core section for isotopic analyses. Sediment samples were dried for at least 24 hours in a LabConco Freezone 4.5 L freeze dryer, then ground and homogenized using a small ball mill (Dentsply Rinn Wig-L-Bug multispeed grinder). Subsamples from every 2nd centimeter of the core were taken for N/S analysis were massed into 3.5x5mm tin capsules, sealed and pressed to remove atmospheric nitrogen. Subsamples for C were massed into 3.2x4mm silver capsules and acidified via fumigation to remove inorganic carbon (Harris et al. 2001), then dried at 60℃ overnight. A combustion aid was added (WO3) and the samples were sealed in tin capsules. Analyses were conducted using continuous flow elemental analysis/isotope ratio mass spectrometry (EA/IRMS). Standard reference samples were measured, and isotopic ratios were expressed in standard format relative to VPDB, AIR, and VCDT. Three replicates of four international isotopic standard reference materials with were analyzed at the beginning of each batch of samples (maximum 150 a day). The reference materials were chosen to provide a range of values that would include the unknown samples. The standards used include: one depleted in ^{15}N and ^{13}C (USGS40), enriched in ^{15}N and ^{3}C (USGS41a), depleted in ^{34}S (IAEA S-3) and enriched in ^{34}S (IAEA S-2). The known elemental concentrations of the standards were used to calculate an acceptable amount of the target elements similar to that of the unknown samples. Final daily correction factors were determined based on the daily analyses of these standards using the following linear regressions:

–4.52 ‰ = m × δ15NUSGS40-workingrefgas + b

+47.55 ‰ = m × δ15NUSGS41a-workingrefgas + b

–26.39 ‰ = m × δ13CUSGS40-workingrefgas + b

+36.55 ‰ = m × δ13CUSGS40-workingrefgas + b

+22.62 ‰ = m × δ34SIAEA S-2-workingrefgas + b

–32.49 ‰ = m × δ34SIAEA S-3-workingrefgas + b

where the values on the left side of the equation are the assigned value of the standards; the δworkingrefgas is the mean daily delta values of the respective international reference materials relative to the working reference gas; b is the additive correction factor; and m is the expansion coefficient correction factor. If replicates do not agree within acceptable tolerances, they are remade, and the analysis is repeated until acceptable statistics are achieved.

3. Results

3.1 Physical Core

WAL17LC1 has nine sections total containing 841 cm of sediment. The sediment is a dark gray, massive, mud matrix. The sediment is organic rich and throughout the core there is small millimeter sized pieces of shiny flakes which appear to be muscovite. This remains constant until section 9. Around 760 cm deep, the sediment changes from a dark gray color to a reddish-brown color. The grain size increases to a sandy mud and there are three layers of sand each one centimeter thick. The layers appear at 765 cm depth, 768 cm, and 829 cm (Figure 14).

3.2 Isotopic Proxy Data

This study utilizes a total of eight downcore proxy records to test the hypothesis. For the purpose of this study, proxy analysis starts 300 cm down core at the top of section 4. At this depth the median age taken from the age model is 3,689 years. It is important to note that the ages used in this study are all median ages but minimum and maximum ages for each sample can vary up to approximately ±2100 years at the base of the core and ±50 years at the top of the core. Geochemical analyses include $\delta^{13}C$, $\delta^{15}N$, $\delta^{34}S$, %OC, %N, %S, OC/N and OC/S. These records are presented against depth and calibrated age (BP) (Figures 5-12).

3.2.1 Carbon

Overall, downcore $\delta^{13}C$ varies between -28.04‰ and -23.54 ‰. Using the defined intervals for climatic events; YD and HCO, general increasing and decreasing trends are observed (Figure 5). From the interval of 5,000 to 7,000 years $\delta^{13}C$ is decreasing from -24.45‰ to -26.31‰ until approximately 6600 years. After which the value increases to -23.66‰ at the end of the interval, 7,000 years. During this interval, %OC has a similar trend (Figure 6). From 5,000 to approximately 6,400 years, values decrease from 17.00% to 12.50%. Values increase up to 18.25% from 6,400 years to 7,000 years.

$\delta^{13}C$ around 8,000 years ago is -25.53‰ and increases to -24.39‰ around 8,050 years ago and then drops again to -25.54‰ at the start of the 8.2 kiloyear event 8,200 years ago. %OC varies between 14.00% and 15.00% but does drop to 13.49% close to the beginning of the event around 8,163 years ago.

In the defined YD interval, 11,500 to 13,000 years $\delta^{13}C$ varies with no real consistent trend from -28.04‰ to -26.11‰. The %OC does follow a trend, decreasing from 19.55% to 6.23%

3.2.2 Nitrogen

Three different proxies are included in the analysis of nitrogen. $\delta^{15}N$, %N and OC/N. During the period of the HCO, $\delta^{15}N$ consistently fluctuates between 3.75‰ and 2.75‰ (Figure 7). There is one notable fluctuation from 6,129 years to 6,284 where the value increase from 2.68‰ to 3.62‰. %N also has small scale variation but is fluctuating from 1.25% to 1.75% (Figure 8). Around 6,500 years, the range in percentages increases to 1.40% to 1.90% until the end of the interval. OC/N remains relatively constant ranging from 11.00‰ to 9.00‰ (Figure 9).

There is little to no variation seen during the 8.2 kiloyear interval, $\delta^{15}N$ remains 3.20‰ and 3.00‰. Similarly, %N increases by a tenth of a decimal downcore from 1.33% to 1.41% during the interval of 8,000-8,200 years ago. The OC/N ratio during this interval remains around 10.00‰ with little variation.

Nearing the base of the core $\delta^{15}N$appears as a decreasing curve starting at 3.13‰ and shifting to 1.67‰ during the YD interval. %N decreases from 1.68% to 0.54%. The OC/N ratio fluctuates as well but is generally decreasing from 12.26‰ to 8.76‰

3.2.3 Sulfur

Sulfur proxies include $\delta^{34}S$, %S, and OC/S. During the HCO, $\delta^{34}S$decreases from -3.84‰ to -10.63‰ but abruptly increases starting at 6,800 years to approximately -6.60‰ at the end of the HCO interval (Figure 10). %S generally increases from 0.60% to 0.87% (Figure 11). OC/S trends in a decreasing fashion from 30.00‰ to 29.68‰ (Figure 12).

Sulfur during the interval of 8,000 to 8,200 cal years BP ranges between -7.49‰ and -8.11‰ with no significant trend. %S ranges between 0.79% and 0.90% with no significant trend. OC/S has a small peak of increasing from 16.83‰ to 19.31‰ around 8,050 years and decreasing to 17.82‰ at 8,200 years BP.

During the YD interval, $\delta^{34}S$drastically increases from -5.74‰ to 3.57‰. %S shows varied trends. From the start of the interval to approximately 12,000 years, %S increases from 1.20% to 1.91%. It then decreases to 0.55% up to 12,740 years when it increases again to approximately 1.10% at 12,860 years and drops down to 0.37% at the end of the YD interval. OC/S during the YD starts in a decreasing trend from 15.09‰ to 4.32‰ at 12,860 years and then increases up to 15.86‰ at the end of the interval.

3.3 Statistical Analysis

In order to better understand the large quantity of data, a correlation matrix was made using the program Past. (Table 1) Strengths of relationships are determined by 99% and 95% confidence intervals. Meaning that a relationship with a P value less than 0.01 has 99% confidence and P values between 0.01 and 0.05 are 95% confident. Mostly all of the proxies had 99% confident relationships except for the relationship between %N and %S as well as OC/S and $\delta^{34}S$. Those two relationships fell within the 95% confidence range. Three proxies did not have significant relationships; %S and $\delta^{15}N$, %S and %OC, lastly OC/N and $\delta^{15}N$. Out of all these, four relationships have very strong R values. The R value is the correlation coefficient. A strong R value is defined as ±1 and a weak R value

is 0. The relationships between $\delta^{15}N$and %OC, $\delta^{15}N$ and %N, %OC and %N, and OC/S and %N are all strong positive relationships.

3.4 Principal Component Analysis

The program Past was also used to create a Principal Component Analysis (PCA). The purpose of this is to summarize the bulk variance in the dataset. A series of principal components are calculated based on eigenvalues. This information can show us which proxies are influences different groups of data (Figure 13). Principal component (PC) 1 and 2 make up approximately 75% of the data's variance. (Table 2) The proxies responsible for PC1 are largely attributed to %N and %OC but also $\delta^{15}N$, $\delta^{13}C$and OC/S. PC2 is driven by %S, $\delta^{34}S$, OC/N and OC/S. In both PC1 and PC2, each of these proxies have moderately strong positive R values with the exception of $\delta^{34}S$and OC/S in PC2 which have moderately strong negative R values (Table 3).

4. Discussion

4.1 Carbon Interpretations

Carbon trends, overall, match what I expected. The stable isotope ratio values during the HCO are higher than during the Younger Dryas. This is consistent in terms of productivity in the water column. However, there is no clear evidence of which plants are being photosynthesized between C_3 and C_4 pants and thus it the best conclusion is that a mix of these plants are making up the organic matter deposited in the sediment (Meyers and Terranes, 2001). The composition of the sediment core shows a physical relationship to the value of %OC downcore, as expected. At the top of section 4, organic carbon percentages range between 10.00% and 15.00% but rapidly decrease in the base of the core to 5.00% and less. During the cold, arid climate of the Younger Dryas, less organic matter is to be expected because plants typically do not grow in those conditions. These results are also consistent with the physical core data where the texture of the core at the base does not appear to be an organic rich dark grey mud but instead a coarse grain terrestrial sediment that has been oxidized (Figure 14). Results from the correlation matrix show that %OC and $\delta^{13}C$have a somewhat strong and significant relationship. (Table 1) This

relationship agrees with the suggestion that the organic carbon in the system comes from different sources. But, it does not explain all sources of carbon deposited in the sediment.

4.2 Nitrogen Interpretations

$\delta^{15}N$shows a similar trend to $\delta^{13}C$in that values during the HCO are higher than during the YD. Values in the low positive numbers lead me to believe that the main plant type source is terrestrial land plants. During the HCO, $\delta^{15}N$ range between 3.00‰ and 4.00‰; according to Meyers and Lallier-Verges (1999), $\delta^{15}N$ for terrestrial plants will be near 0.00‰. I interpret this as a mix of terrestrial plants and nitrate dissolved in aquatic plants existing during the HCO but only terrestrial plants during the YD. This interpretation is also consistent with the climate conditions of each event and the preferred growing conditions for vegetation. While the more probably source for vegetation during the Younger Dryas is terrestrial plants, the percentage of nitrogen in the sediment overall is low during this interval with values falling under 0.50%. During the HCO, %N falls between 1.00 and 1.50. This leads to the interpretation that less vegetation was being deposited during the YD than the HCO. The OC/N values during the HCO have minimal variation and value at 10.00‰. This shows that the source of organic matter came from a mix of land and aquatic plants. During the YD values appear to fall in the range of the aquatic plant source (Meyers and Terranes, 2001). This is inconsistent with the interpretation given by the $\delta^{15}N$. However, with the lack of plant growth during the Younger Dryas it is still possible to have a mix of land and aquatic plants as seasonality still existed. Perhaps the deposition of plant matter was on a lesser scale overall.

4.3 Sulfur Interpretations

Due to some sampling errors, the sulfur record is not entirely complete, and some data is missing. My expectations do align with the data that does exist. In the HCO interval there is an increasing $\delta^{34}S$values from negative to low positive. The increasing value can describe increased mixing in the water column and can be indicative of sulfate reducing conditions. During the YD we see increased $\delta^{34}S$. This is consistent with increased mixing

within the water column which makes sense for the beginning of the lakes history when it was shallow and existed during dry windy conditions. The isotopic data correlates well with the physical core data as the base is highly oxidized unlike the rest of the core.

4.4 Principal Components

Using the program Past, a Principal Component Analysis (PCA) was done to understand the variation in the dataset. PC1 and PC2 (Figure 15) make up 75% of the variation in the data (Table 2). The PCA plot groups together each climatic event in 95% ellipses (Figure 13). PC1 components show they are mostly driving the HCO where PC2 components drive 8.2 Kiloyear and YD. It is also noted that the 8.2 Kiloyear ellipses falls within that of the YD which makes sense since they are similar climatic events. PC1 is made up of %OC and %N and respectively $\delta^{13}C$and $\delta^{15}N$. PC1 explains 48% of the variance. I am interpreting principal component 1 to explain productivity in the water column as carbon and nitrogen relate to this. Higher values can be interpreted as more productivity where lower values relate to less productivity (Figure 16). This plot shows that productivity is higher during the HCO and lower during the YD. PC2 is composed of $\delta^{34}S$and %S, this is related to the hypoxic and anoxic conditions explaining the majority of the variation in the record at this time (Fig 13) PC2 explains approximately 27% of the variance in the core. PC2 values are lower during the HCO and higher during the YD (Figure 17).

4.5 The 8.2 Kiloyear Event

Though significant changes are recorded during the HCO and YD, it is difficult to interpret variations within the 8.2 Kiloyear Event. Based on the current understanding of this event, I would expect values to appear similar to those of the YD but on a smaller scale. It is not evident that such values are visible within the designated interval. However, with the disclaimer in mind that the age intervals designated to each paleoclimatic event during this research are based on the median age of this model and that there is room for error, it is possible that the 8.2 Kiloyear event may have happened deeper in the core. After

reviewing the records again consistent abrupt changes appear at 632 cm and again at 638 cm depth in the $\delta^{13}C$ and $\delta^{15}N$. These depths are assigned the ages 8,300 years cal BP and 8,537 years cal BP. These abrupt changes are similar to the changes of the YD but on a smaller scale and if the 8.2 Kiloyear event is existing deeper in the core, then the YD may also be starting deeper in the core. Between the $\delta^{13}C$ and $\delta^{15}N$, recorded depths for the start of the potential YD interval are 827 and 829 cm. The age assigned to these depths are roughly 13,450 years cal BP. With the understanding that there is consistent evidence for the start of these events happening deeper in the core than my assigned intervals this leads me to believe that the age model is not completely accurate. As mentioned before, the ages assigned to each depth is based on the age median between the possible minimum and maximum ages. Because the age model is based on a bulk carbon dating, I would like to propose a potential 300-year carbon reservoir correction. Since it is not likely that Walden Pond experienced a global event 300 years before the rest of the world, it makes sense to say that the median ages are approximately 300 years older than their actual ages. Within the physical core there are three sand layers anomalous with the YD and the deepest layer exists at 829 cm. Using the event stratigraphy, it can be said that the start of the YD is at 829 cm deep in the core. Using this correction, the 8.2 Kiloyear Event shows an abrupt decrease in the $\delta^{13}C$ proxy at around 628 cm deep and at 632 cm, the lowest $\delta^{13}C$ value is -26.38‰. The values increase drastically to -24.41‰ at 638 cm depth or what I have newly defined as the start of the 8.2 Kiloyear event. The changes in $\delta^{13}C$ are consistent with YD responses on a smaller scale as I expected.

4.6 Spectral Analysis

A spectral analysis was run on all proxies as well as PC1 and PC2 (Figures 18-27). The results can be seen in table 4. A few takeaways from this are significant centennial cycles. Figures 18 through 27 show each of the analysis and 99%, 95% and 90% confidence intervals. A table created by S.C. Clemens (2005) highlights different centennial scale solar variability cycles that my data falls within. (Table 4) PC1 shows strong evidence for cycles happening between 200 and 230 years which could likely be explained by sunspots. (Figure 26) PC2 has stronger evidence for 120-150-year cycles which is different from the solar variability and is thus, currently unknown. (Figure 27)

5. Conclusions

Walden pond endured a significant amount of climate change since being created. The purpose of this study was to test the hypothesis that Walden Pond is sensitive to regional and hemispheric climate change bracketed by the Younger Dryas and the Mid Holocene Climate. During the HCO, productivity is higher, and the source of particulate organic matter is a mix of terrestrial land plants and lacustrine algae and overall organic matter is more abundant. During the YD, there is less organic matter and productivity is lower. Oxidation and reduction conditions are less likely during the HCO where they are higher during the YD. Each of these interpretations are consistent with the understanding of the climate during these events. The HCO is a climatic optimum where temperature was warmer and, precipitation is increased allowing for the growth of vegetation, increase in photosynthesis and increase of productivity in the water column. During the Younger Dryas the temperature is cooler, windier and dry. The lake was shallow and mixing in the water column caused the organic depleted sediment to oxidize. Ice chunks also deposited coarser grain sand layers in the lake. Principal component analyses lead to the conclusion that 75% of variance in the core relates to productivity and oxidation and reduction in the water column. Event stratigraphy within the core in combination with isotopic stratigraphy lead to the understanding that the age model based on bulk organic carbon of 11 AMS radiocarbon dates is approximately 300 years younger than initially believed and could relate to an increased carbon reservoir. Spectral analysis of PC1 and PC2 result in the observation of significant cycles on 250-year scales and some longer period cycles that most likely relate to solar variability. There was also significant evident of a shorter period cycle around 135 and 100 years but the cause of these cycles are currently inconclusive. Future work includes a complete down core record starting at the top of the core rather than section 4. A better understanding on spectral analysis and the cyclic nature of some climatic events will also be a part of future work.

6. Figures

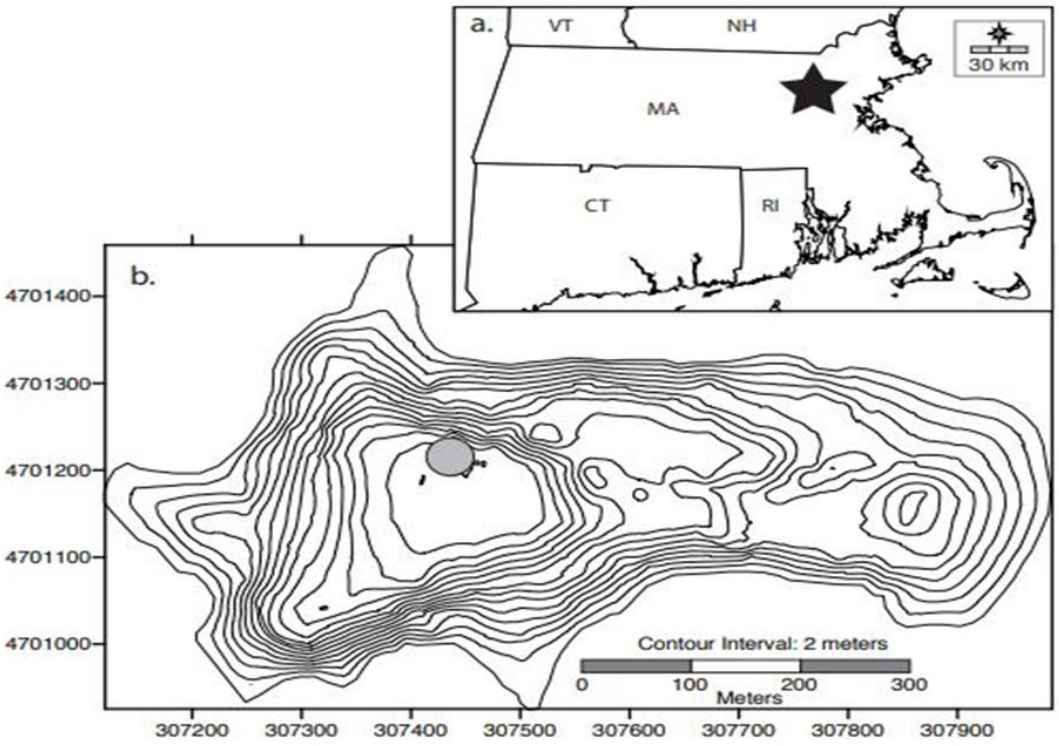

Figure 1 - Modified from Stager et al., 2018. Walden Pond located in Concord, Ma is a closed fresh water body system. Preliminary field work provided subsurface data revealing the deepest basin of the lake. Circle indicates location of Livingstone core.

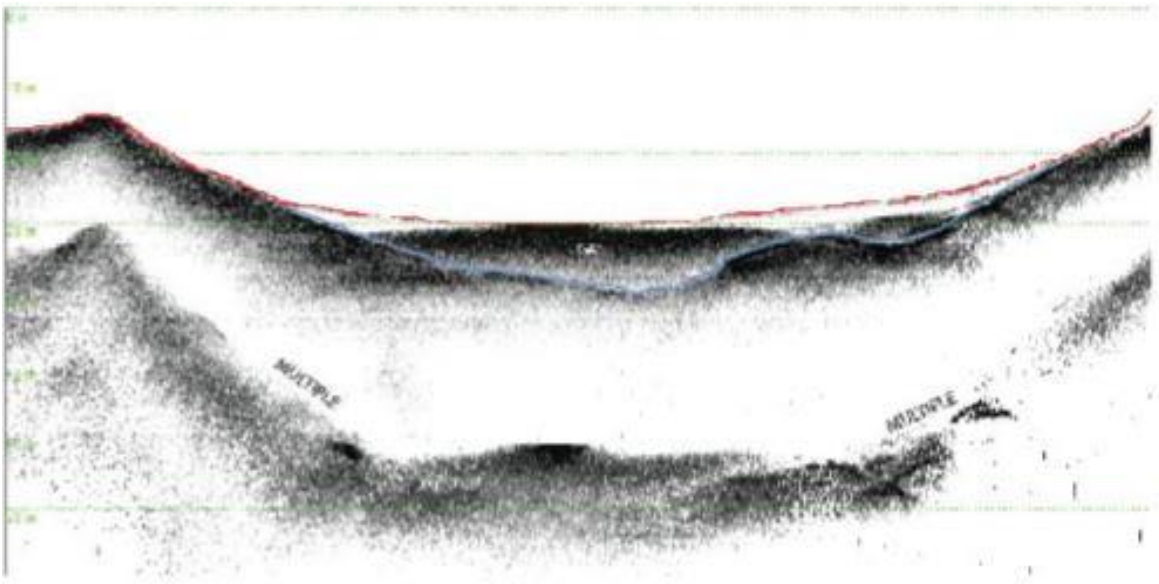

Figure 2 - From Knights et al., 2017. Seismic reflection data from western basin showing >10 m of sediment accumulation at zmax = 30.1 m. Note the gas wipe out at the center of the basin eliminating internal reflectors, which is indicative of eutrophication.

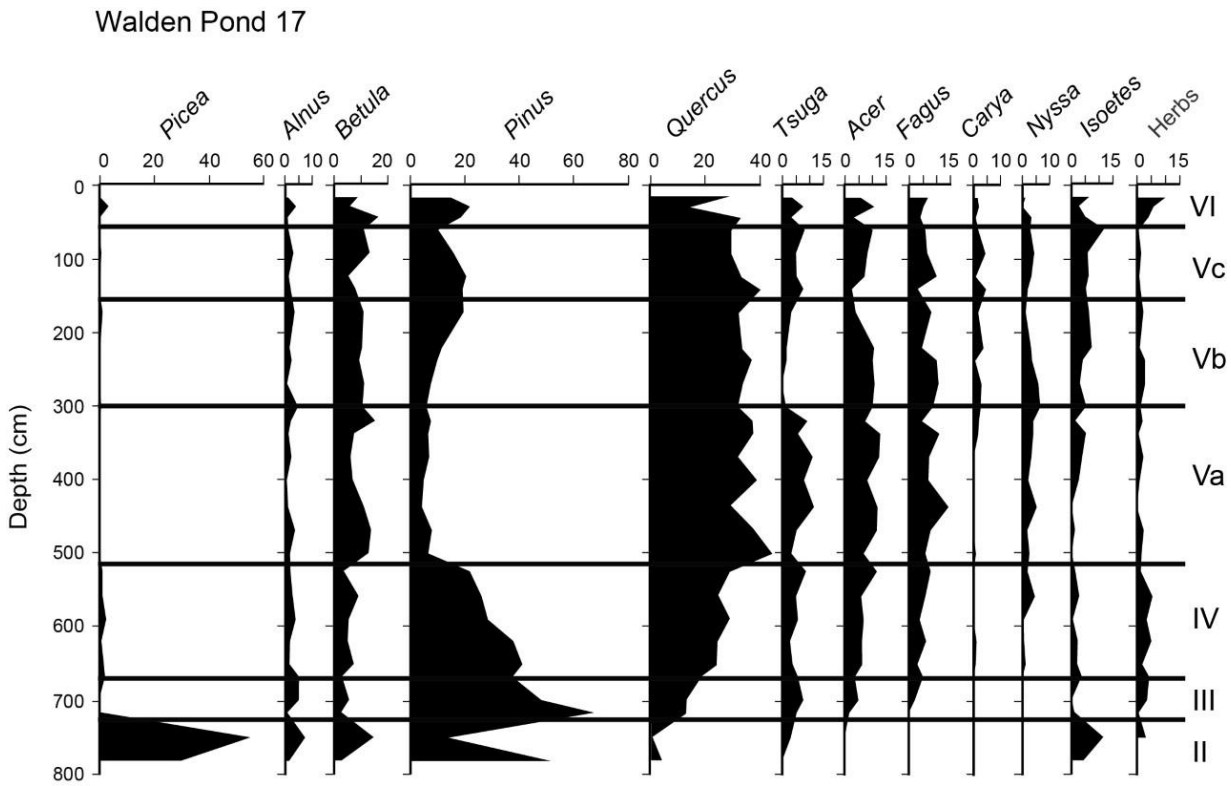

Figure 3 - From Francine McCarthy 2017, downcore pollen data. Quercus (Oak) is most abundant at the top of the core and its maximum abundance is around 500 cm depth where it then starts depleting. Pinus (Pine) is most abundant towards base of the core as well as Picea (Spruce).

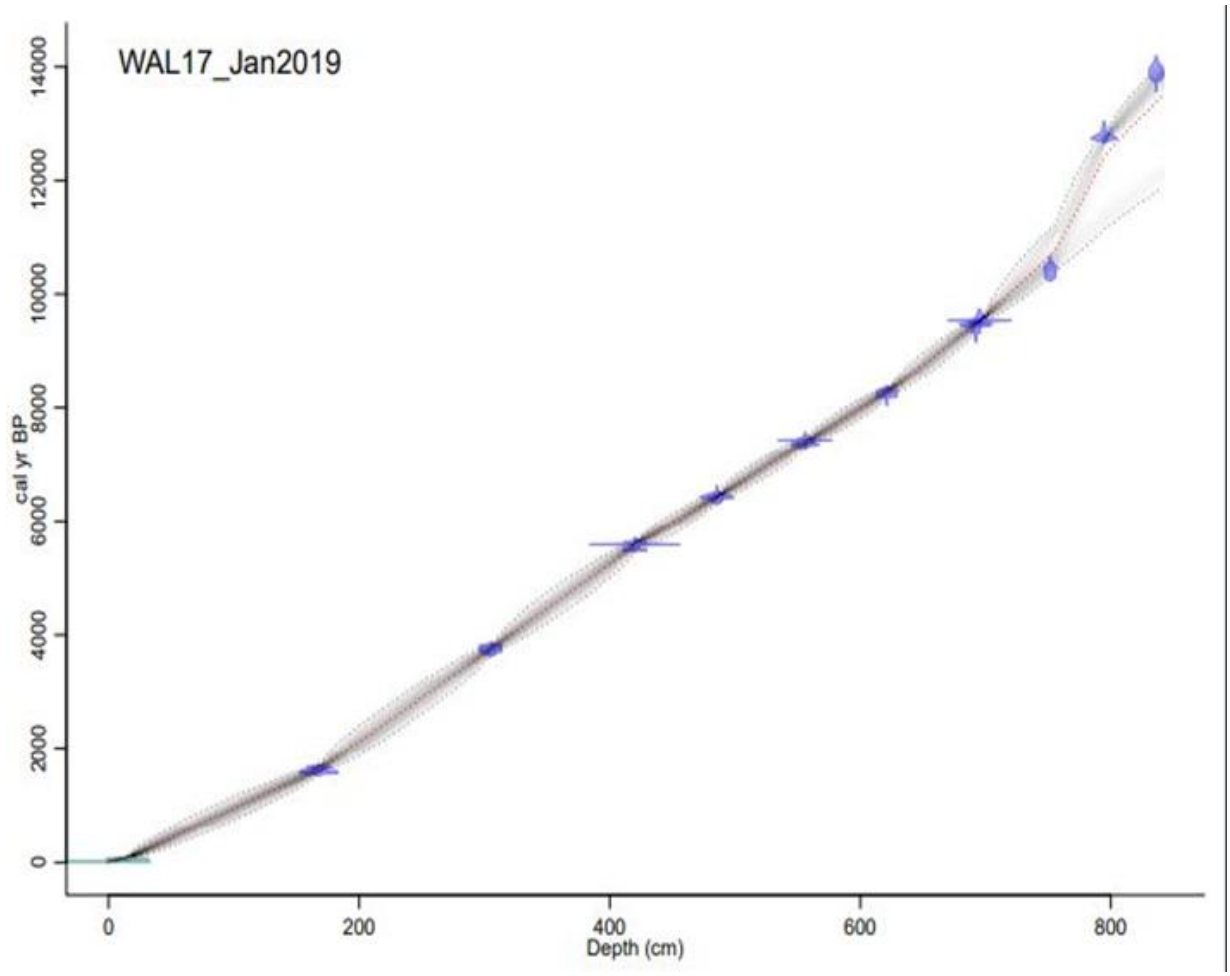

Figure 4 - Age model for whole length of core. Eleven bulk carbon samples were radio dated at WHOI (Marked by blue points).

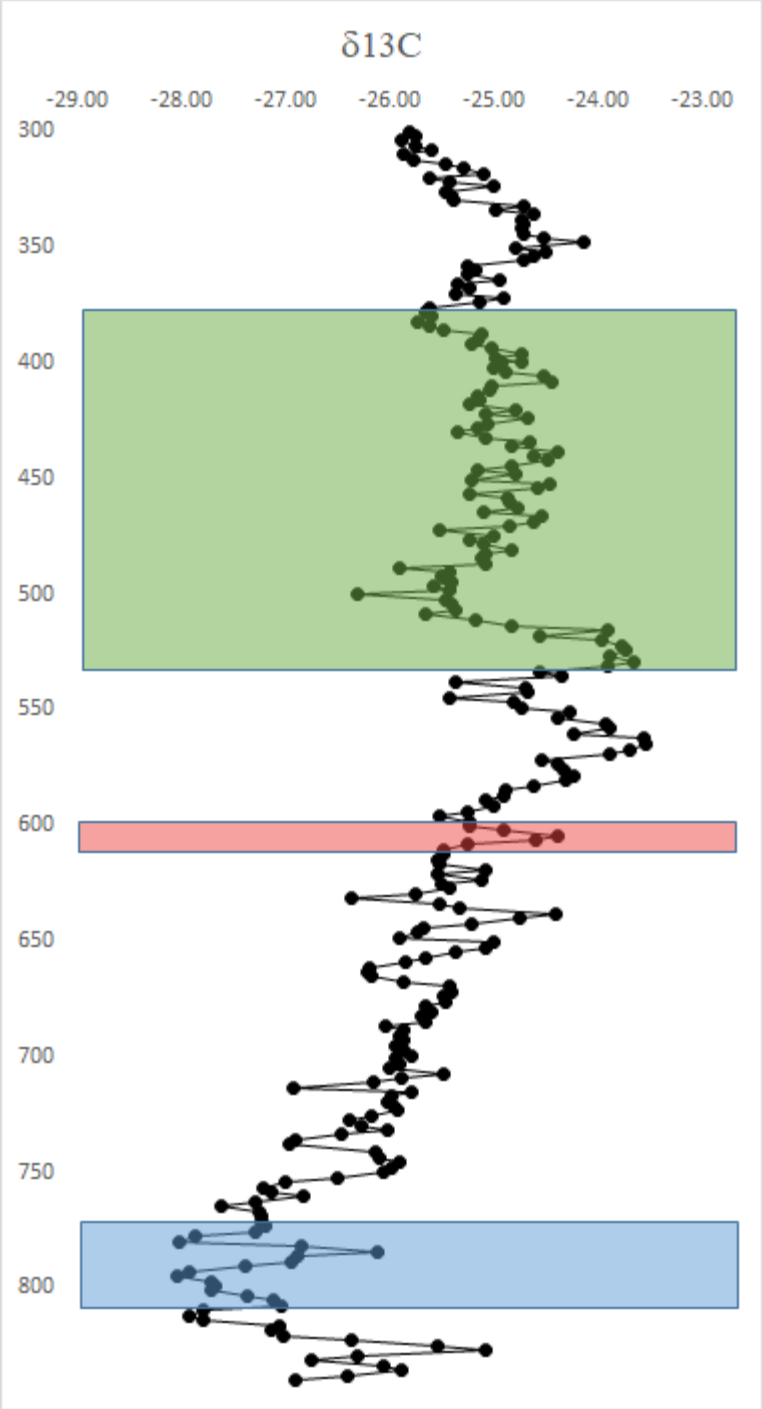

Figure 5 - $\delta^{13}C$ downcore plot vs depth in centimeters. Green shaded region represents the HCO (5,000-7,000 years cal BP). Red region is the 8.2 Kiloyear event (8,000 - 8,200 years cal BP). Blue region is YD (11,500-13,000 years cal BP). Each shaded region is based on age model (Figure 4) before 300-year correction.

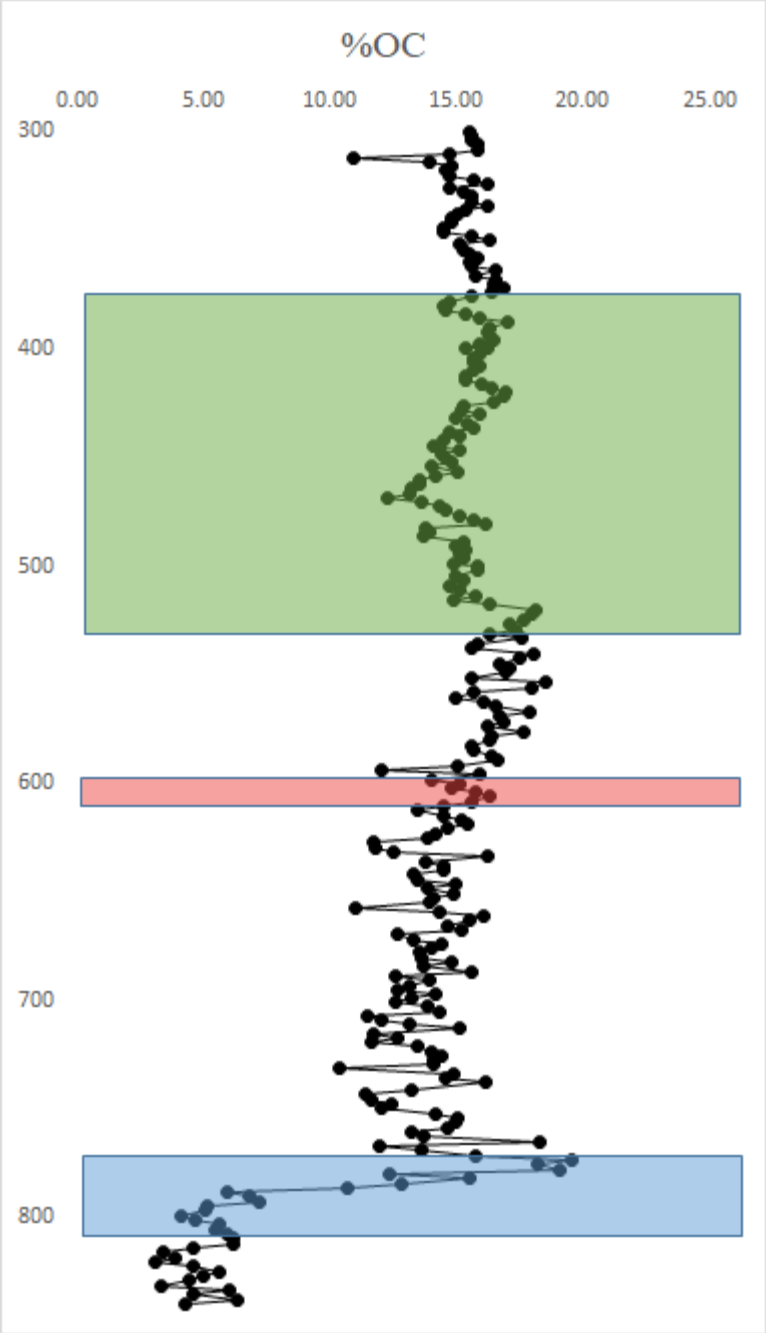

Figure 6 - Percent organic carbon downcore plot vs depth in centimeters. Green region is HCO, red region is 8.2 Kiloyear event, blue region is YD.

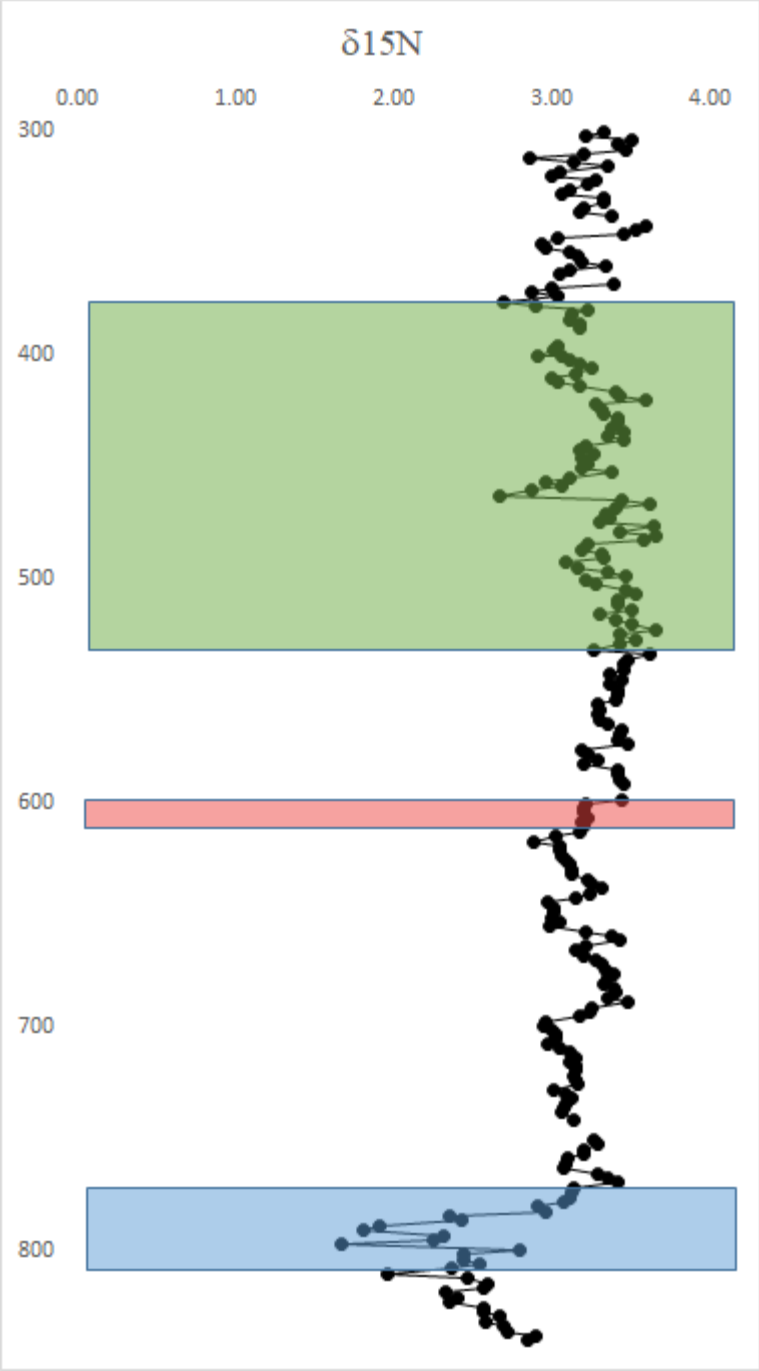

Figure 7 - δ^{15}N downcore plot vs depth in centimeters. Green is HCO, red is 8.2 Kiloyear and blue is YD.

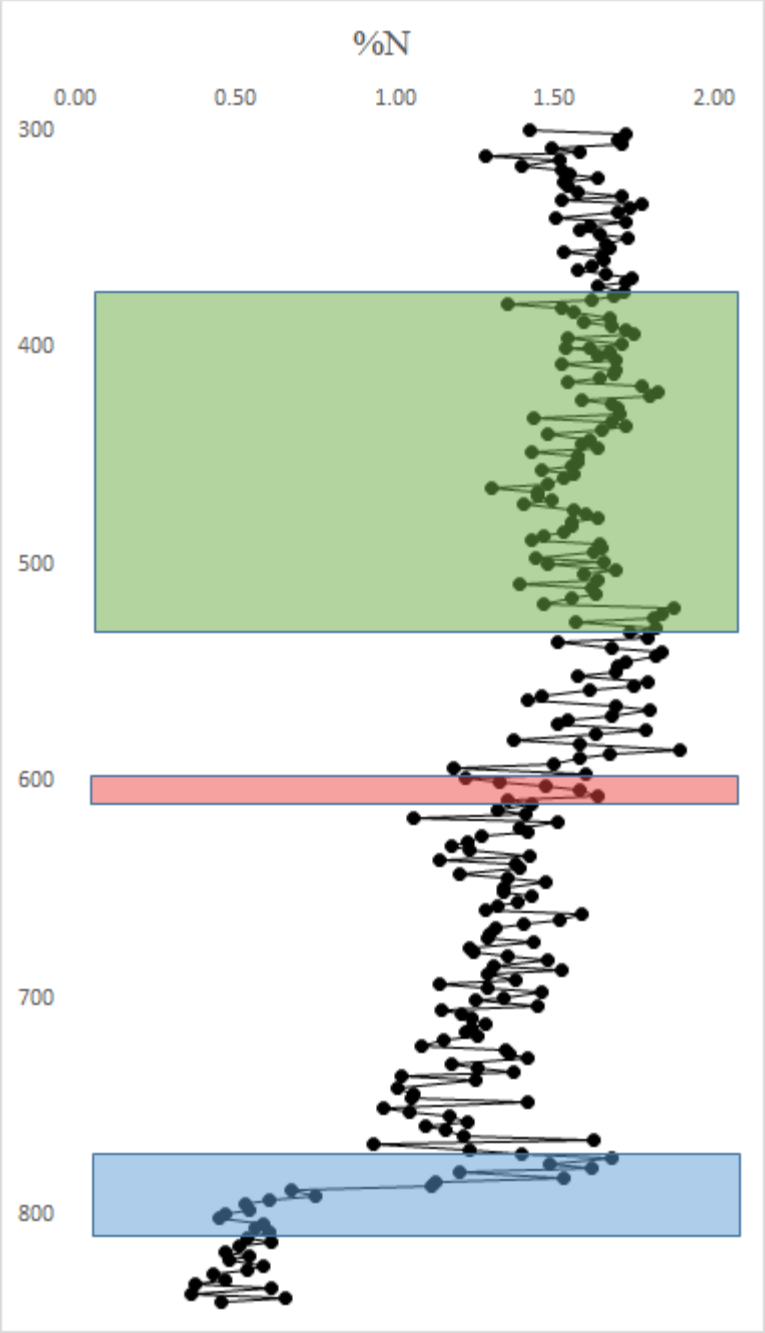

Figure 8 - %N vs depth in centimeters downcore plot. Green is HCO, red is 8.2 Kiloyear and blue is YD.

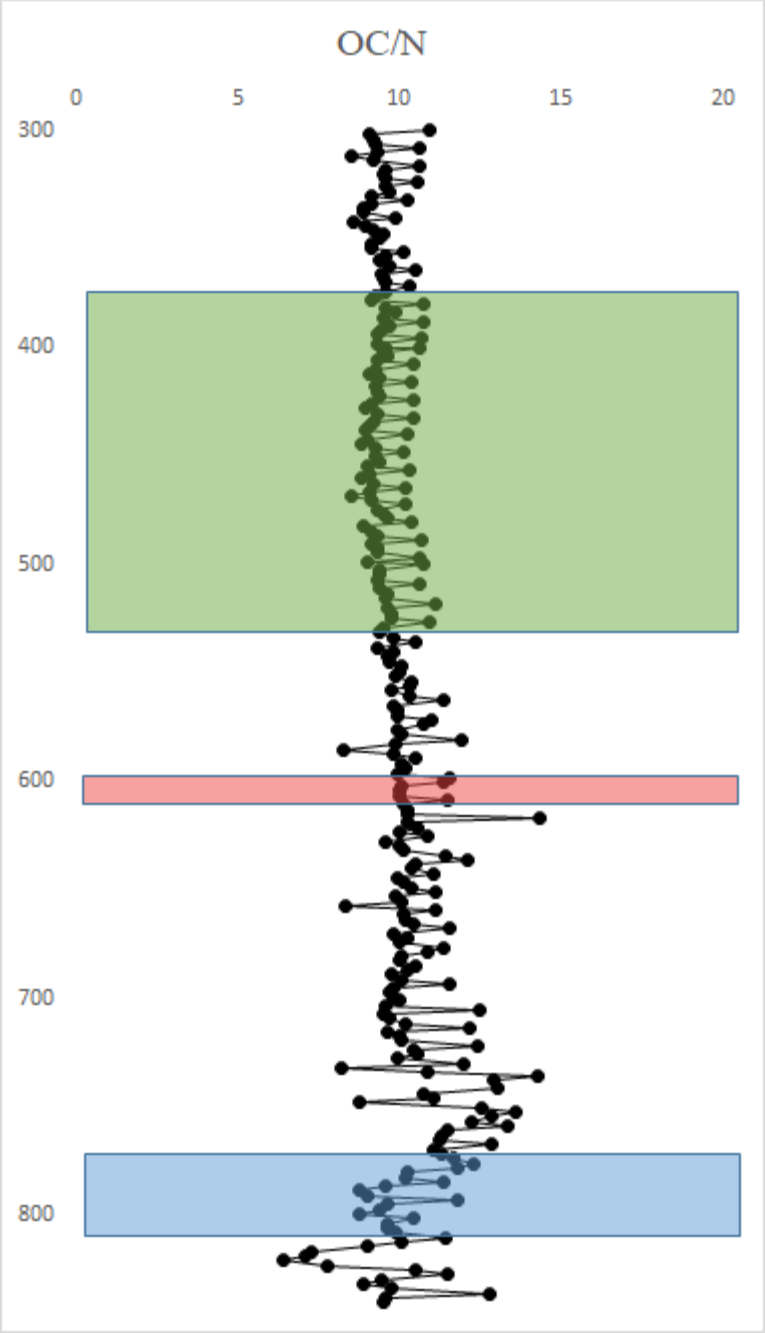

Figure 9 - Organic carbon to nitrogen ratio vs depth in centimeters. Green is HCO, red is 8.2 Kiloyear and blue is YD.

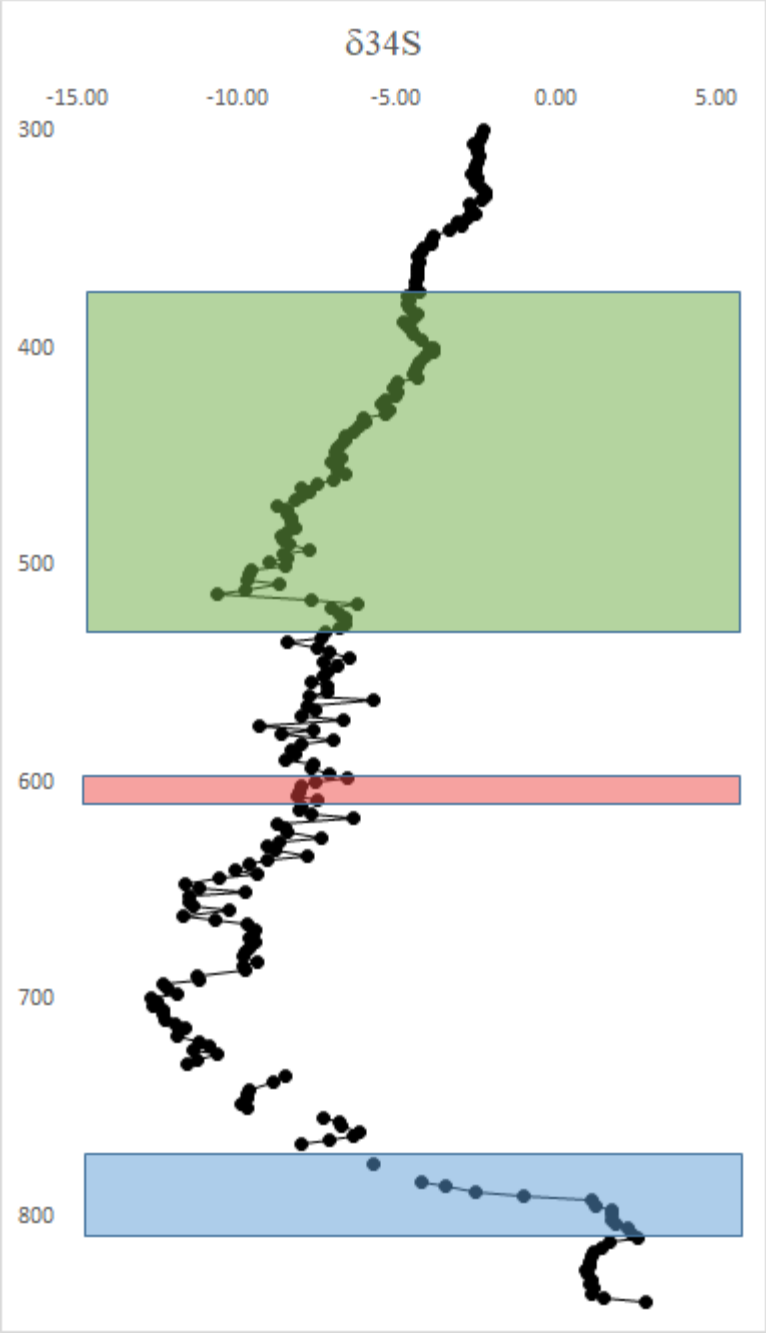

Figure 10 - $\delta^{34}S$ downcore plot vs depth in centimeters. Green is HCO, red is 8.2 Kiloyear event and blue is YD. Spaces in between data points are missing $\delta^{34}S$ values that will need to be resampled.

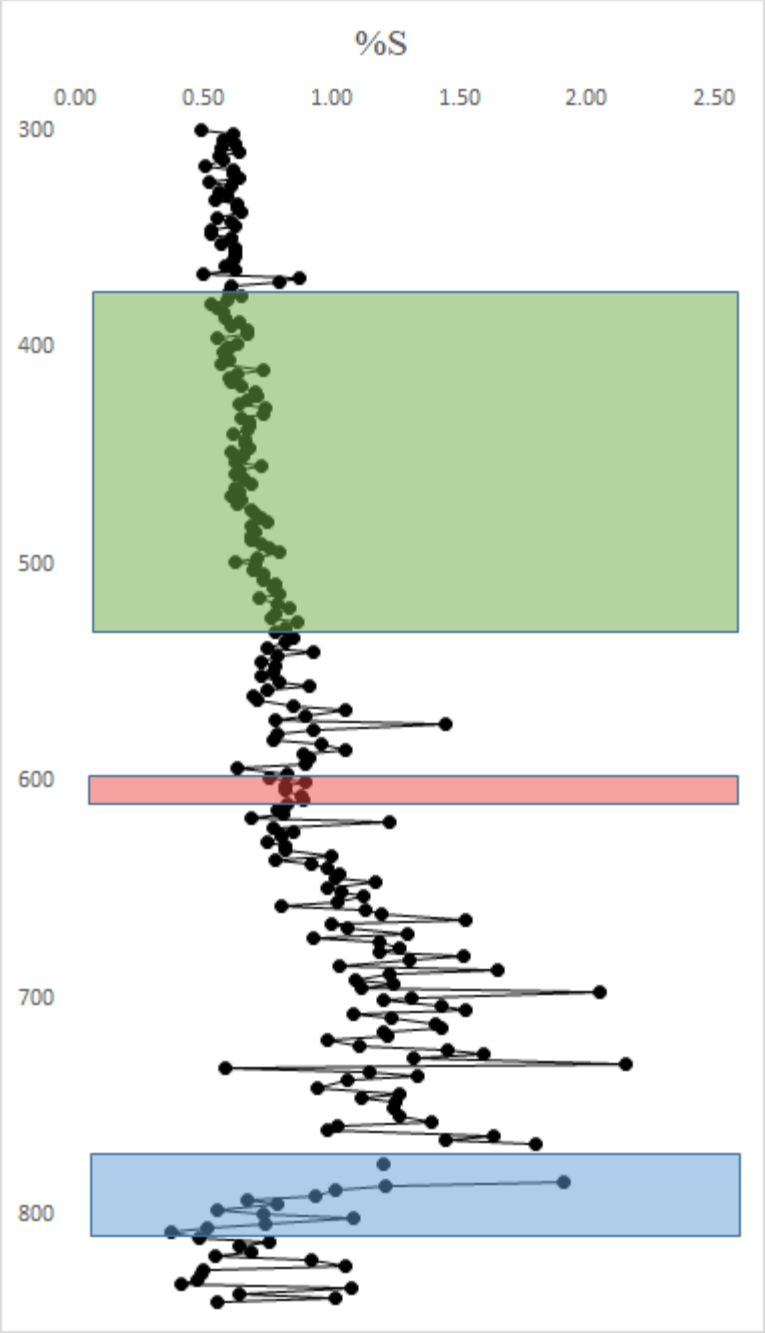

Figure 11 - %S downcore plot vs depth in centimeters. Green is HCO, red is 8.2 Kiloyear event and blue is YD.

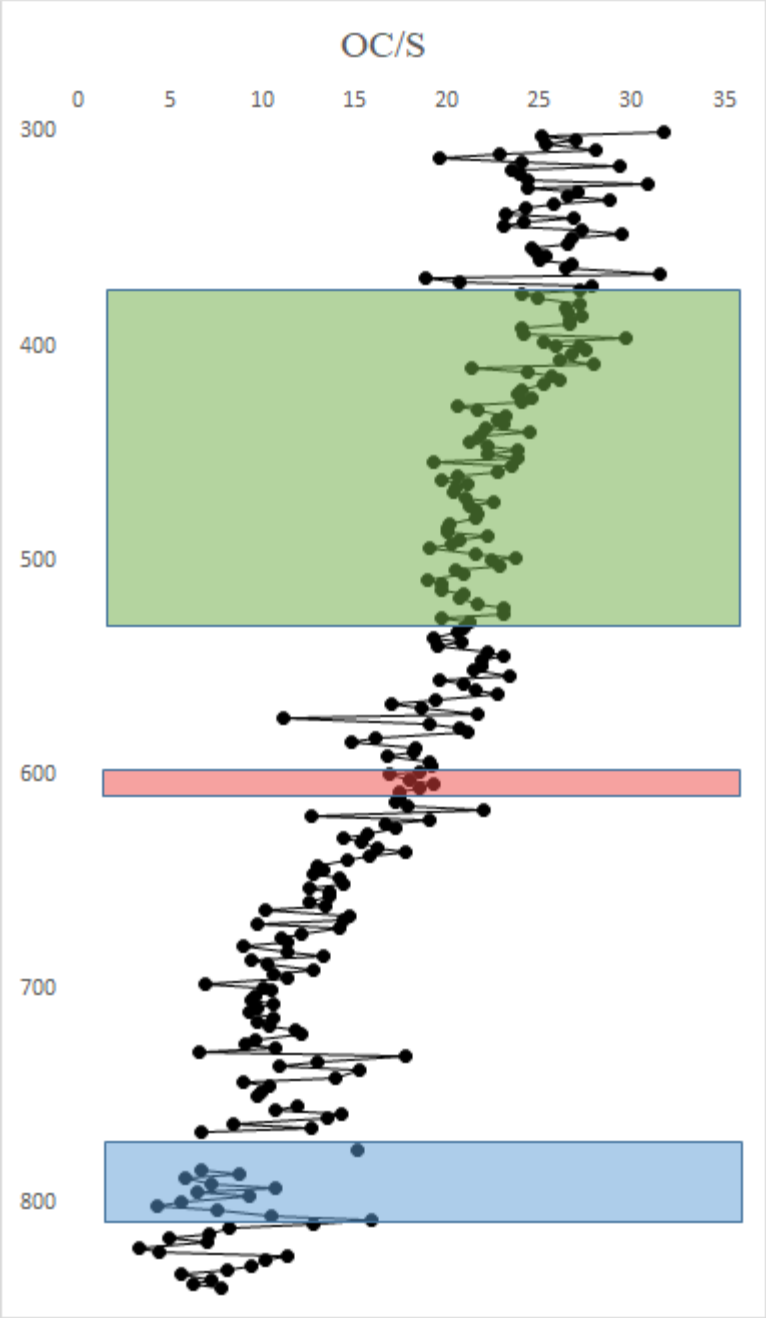

Figure 12 - Organic carbon to sulfur ratio vs depth in centimeters downcore plot. Green is HCO, red is 8.2 Kiloyear event and blue is YD.

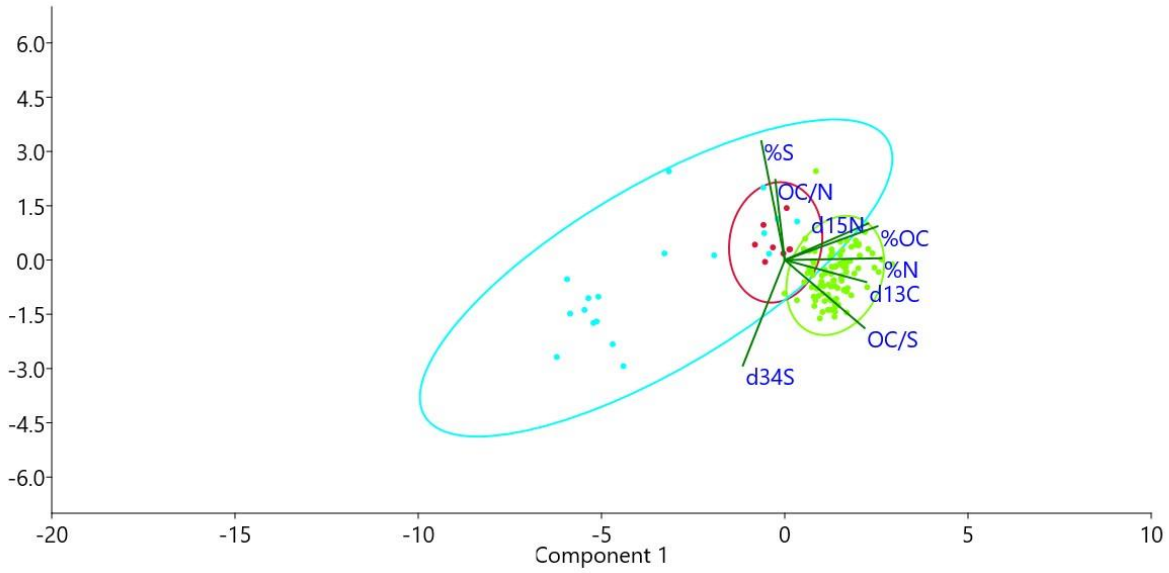

Figure 13 - Principal component analysis plotted in the program Past. Principal component 1 is the x-axis and principal component 2 is the Y axis. Data is grouped by climatic event. Green is HCO, red is 8.2 Kiloyear and blue is YD. The events are grouped by age based on defined intervals before 300-year age correction.

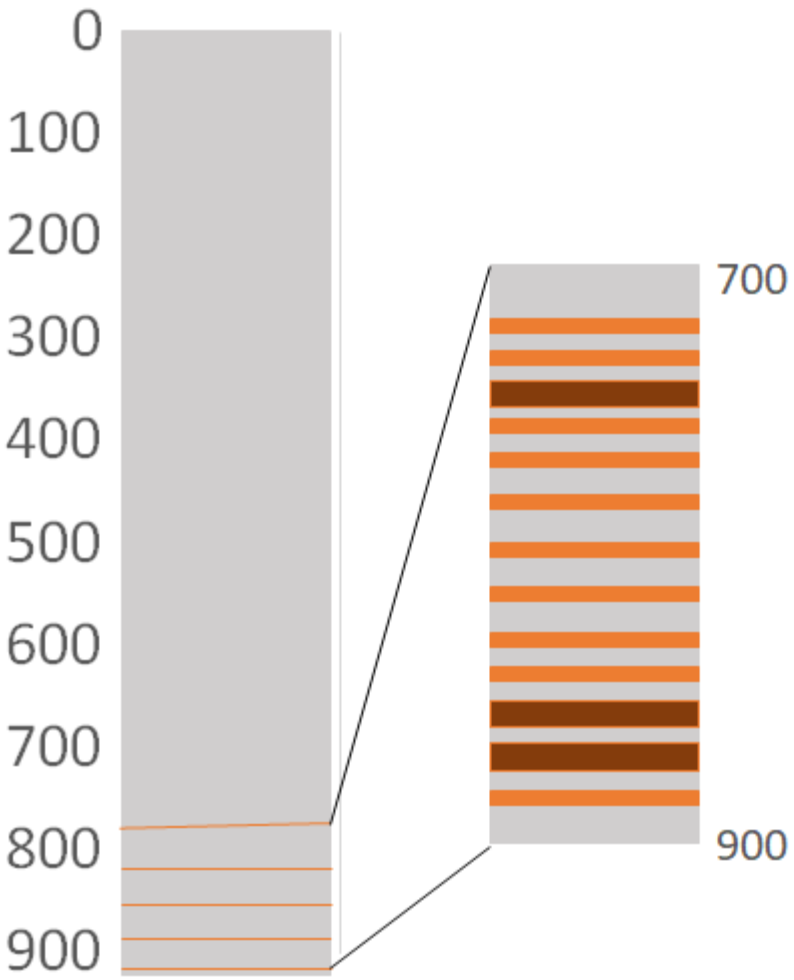

Figure 14 - Basic depiction of core stratigraphy. Matrix is a dark grey organic rich mud with mica flakes throughout. Around 762 cm deep, the mud becomes reddish brown with intermittent oxidized material. Three distinct centimeter thick bands are shown in the zoom in on the figure at 765 cm, 768 cm and 829 cm.

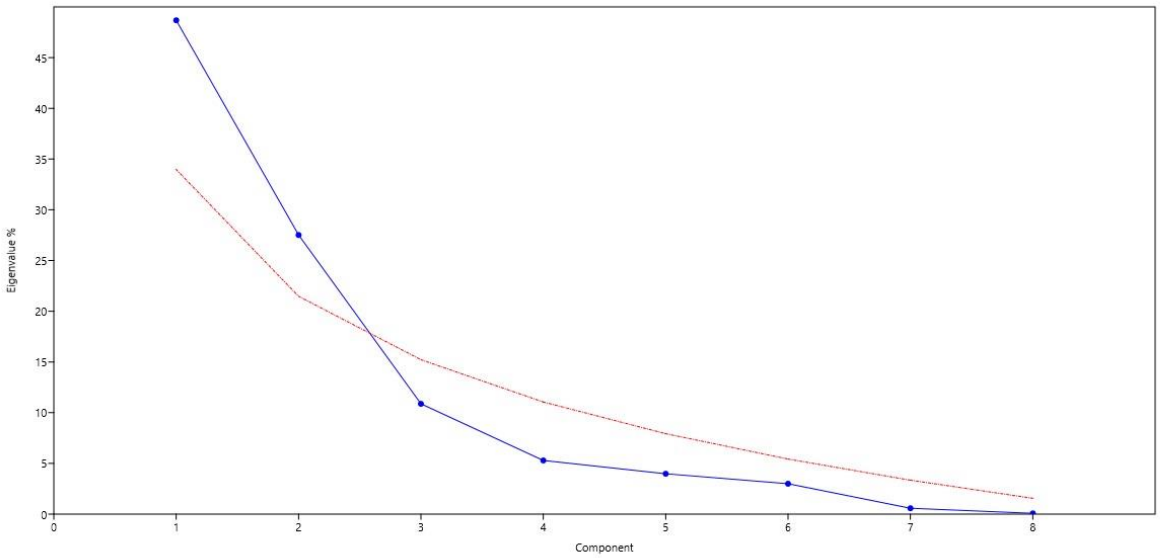

Figure 15 - Scree plot with broken stick (red). This plot shows the significance of PC1 and PC2 as they plot above the red line. This shows each component vs the % eigenvalue.

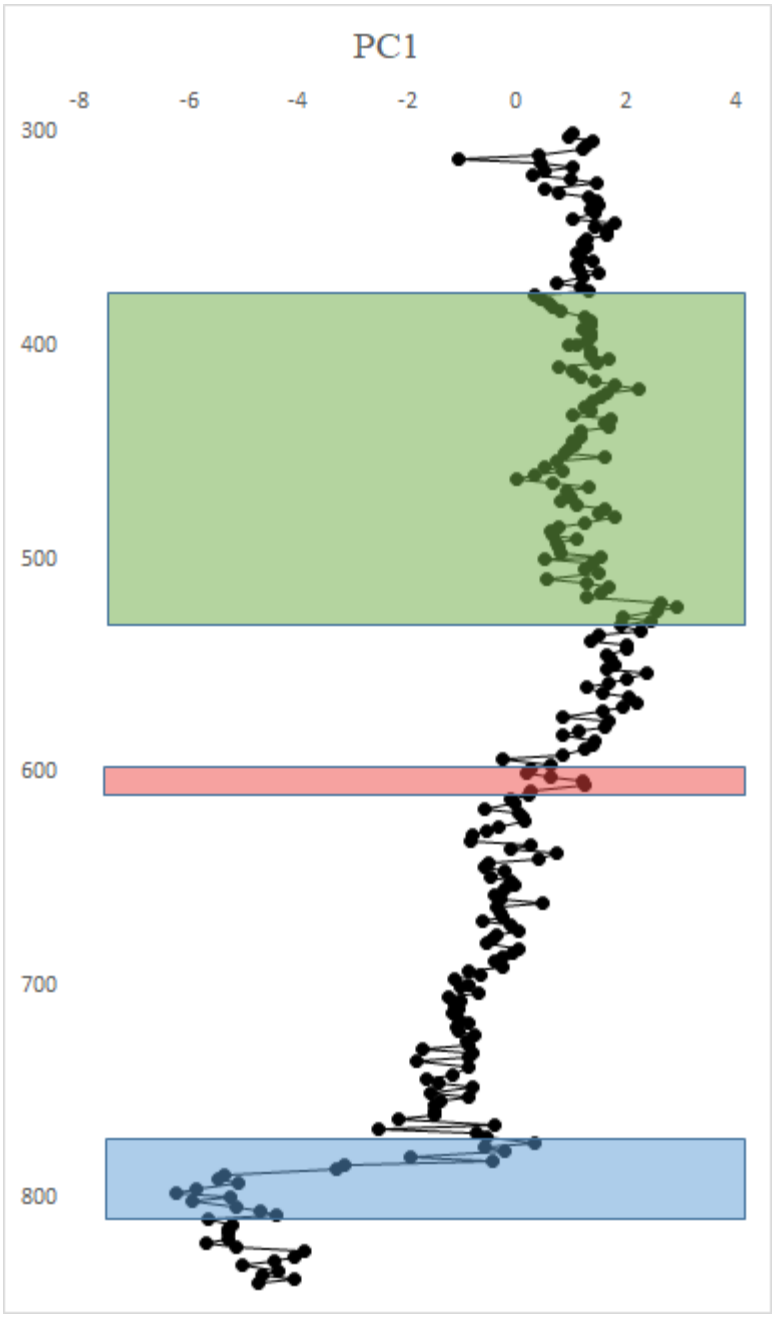

Figure 16 - PC1 loadings vs depth centimeters downcore plot. Values greater than zero can be interpreted as increased productivity where values less than zero can be interpreted as decreased productivity. Green is HCO, red is 8.2 Kiloyear and blue is YD.

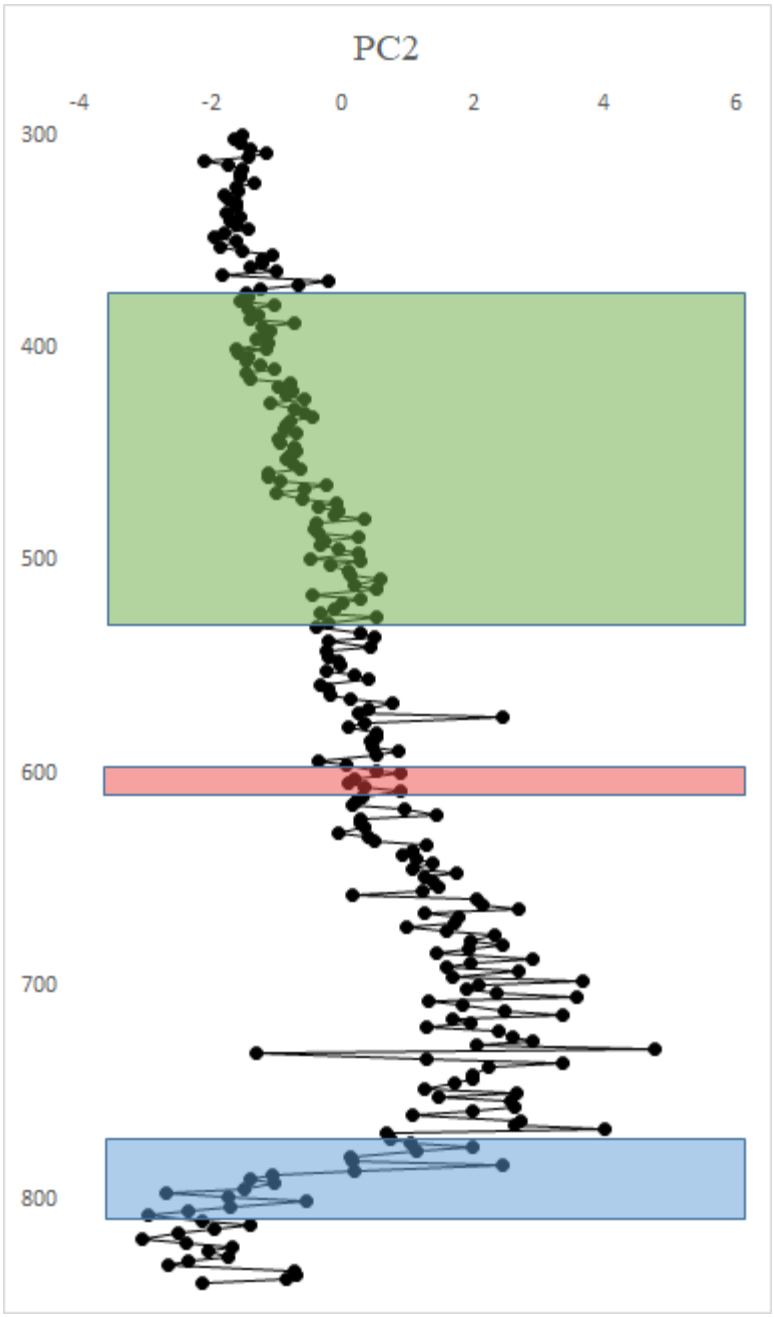

Figure 17 - PC2 downcore plot vs depth in centimeters. Values less than zero can be interpreted as more oxidation - reduction and values greater than zero can be interpreted as less oxidation - reduction. Green is HCO, red is 8.2 Kiloyear and blue is YD.

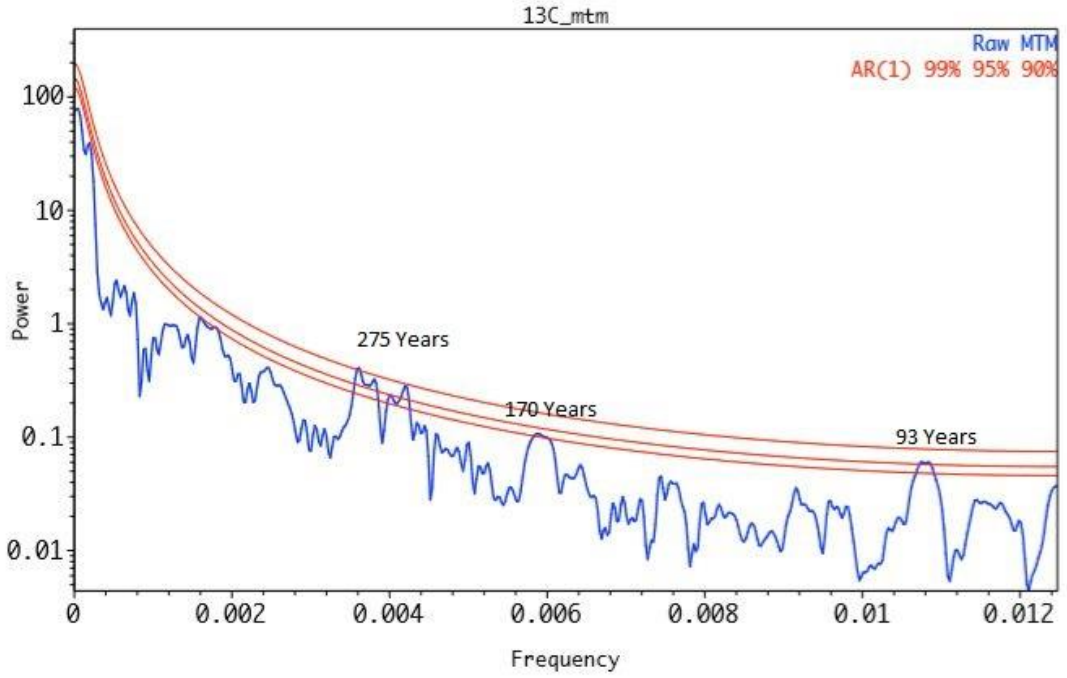

Figure 18 - Spectral analysis of $\delta^{13}C$. Periodicity is labelled at 99%, 95% and 90% confidence intervals. Cycles are observed at 275, 170 and 93 years.

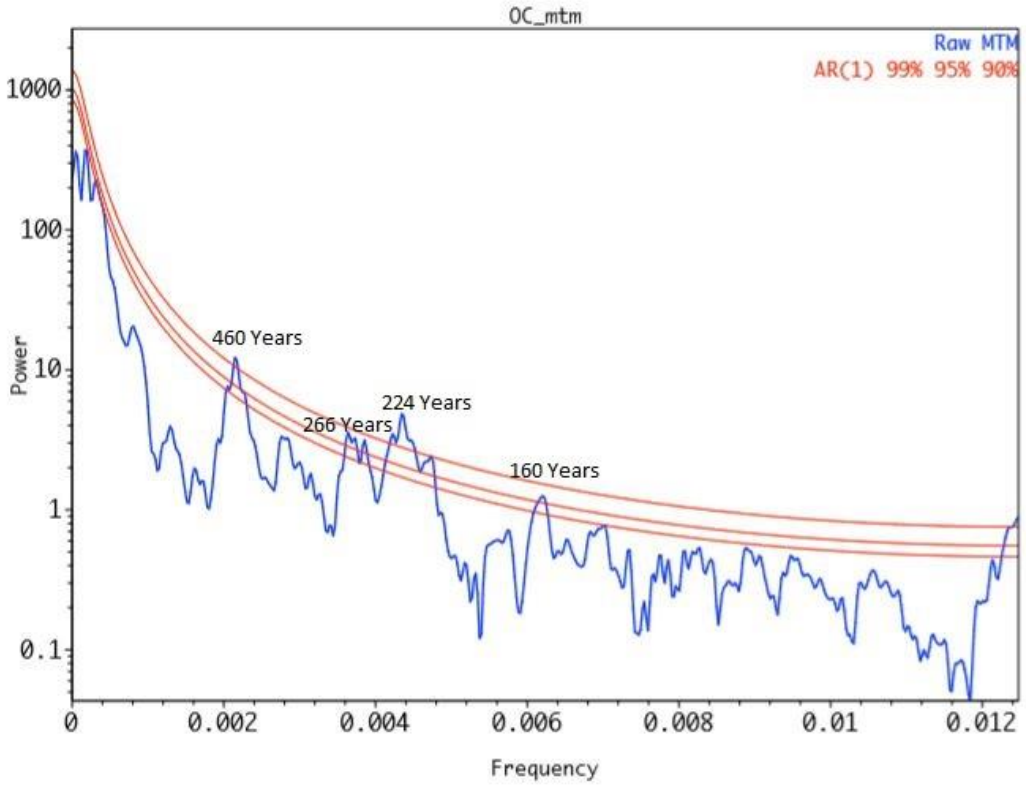

Figure 19 - Organic carbon percentage spectral analysis. Periodicity is labelled at 99% and 95% confidence levels. Cycles are observed at 460, 266, 224 and 160 years.

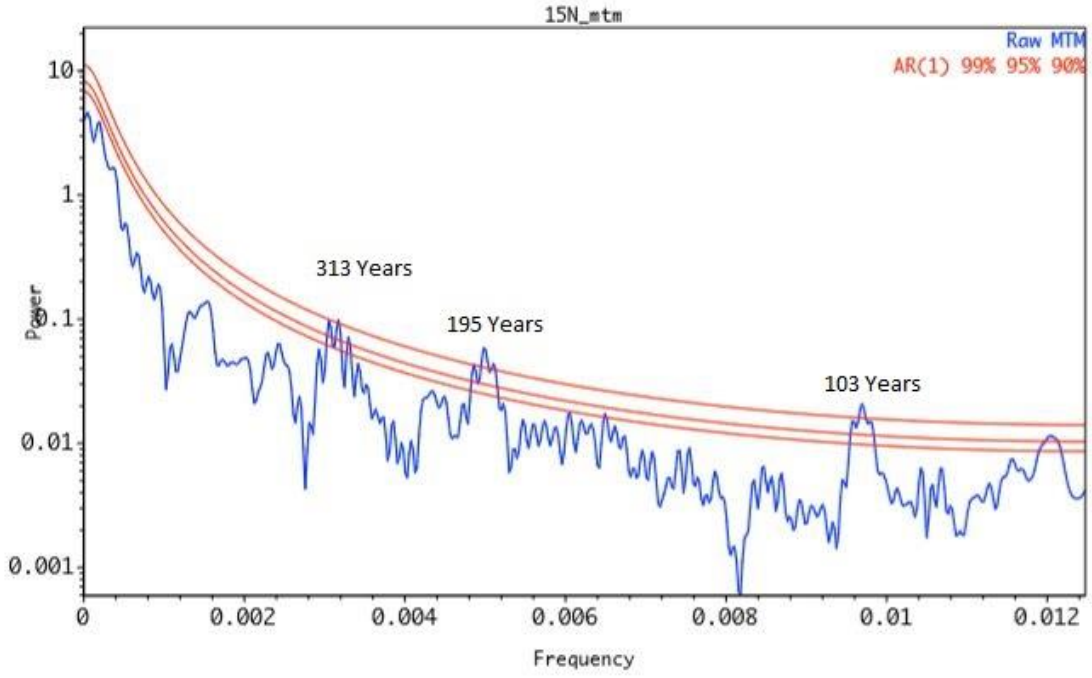

Figure 20 - δ^{15}N spectral analysis. Periodicity is labelled at 99% confidence levels. Cycles are observed at 313, 195 and 103 years.

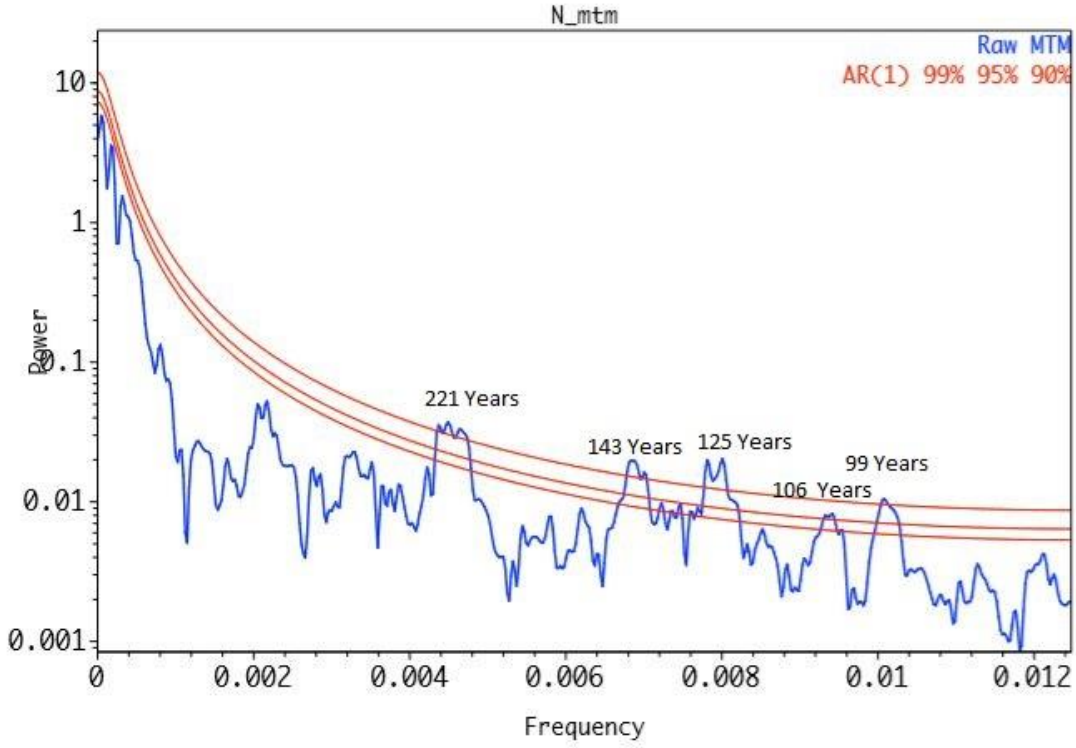

Figure 21- Percent nitrogen spectral analysis. Periodicity is labelled at 99%, 95% and 90% confidence levels. Cycles are observed at 221, 143, 125, 106 and 99 years.

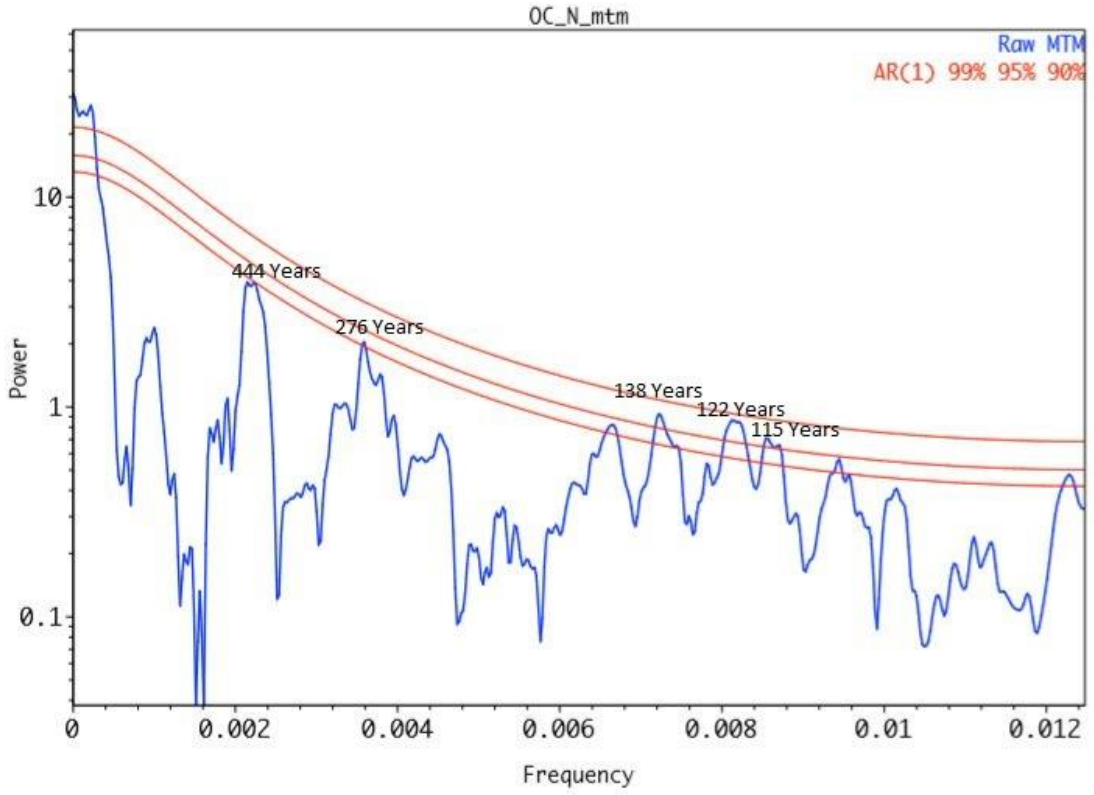

Figure 22- Organic carbon to nitrogen ratio spectral analysis. Periodicity is labelled at 95% and 90% confidence levels. Cycles are observed at 444, 276, 138, 122 and 115 years.

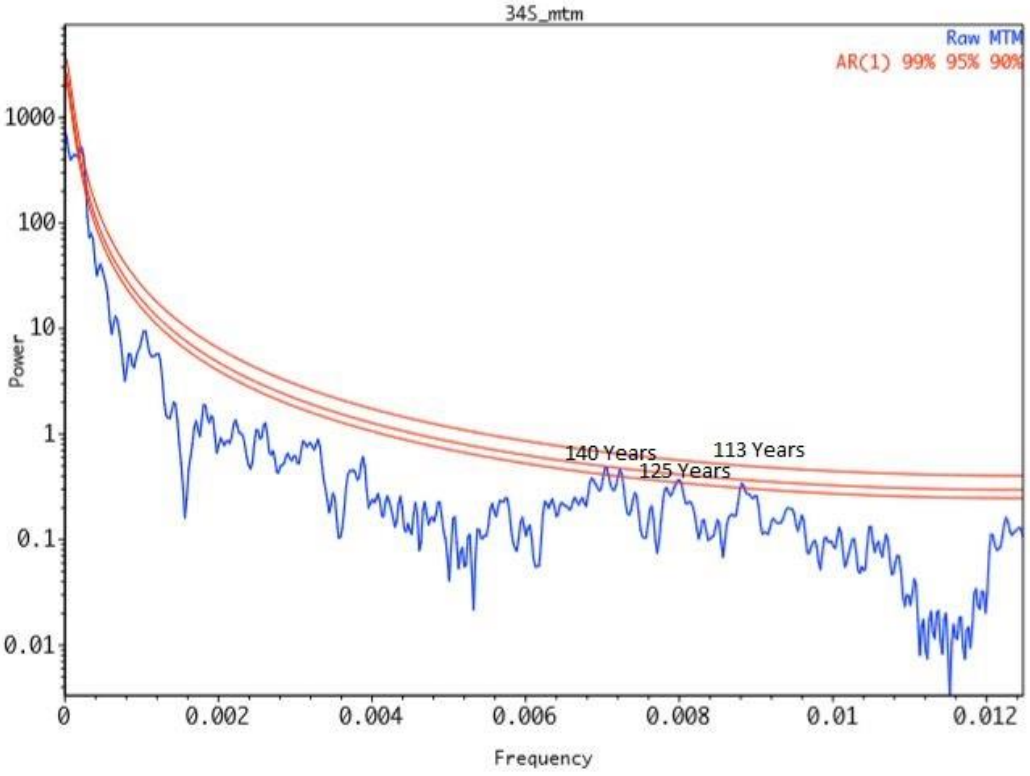

Figure 23 - δ^{34}S spectral analysis. Periodicity is labelled at 90% confidence levels. Cycles are observed at 140, 125 and 113 years.

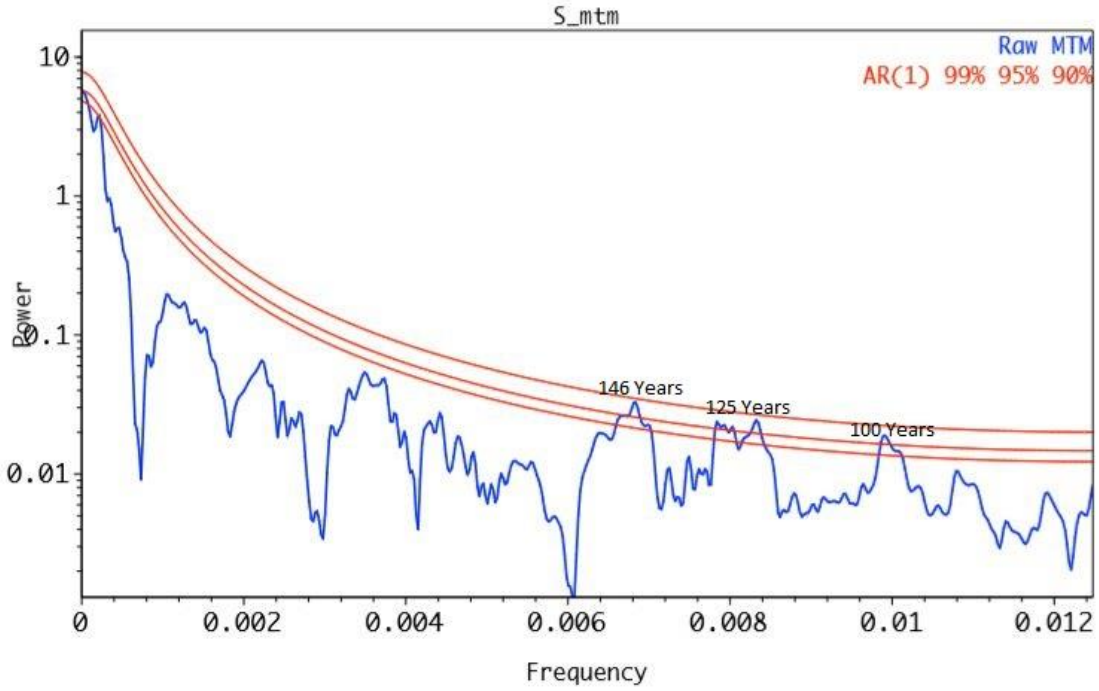

Figure 24 - Sulfur percentage spectral analysis. Periodicity is labelled at 95% and 90% confidence levels. Cycles are observed at 146, 125 and 100 years.

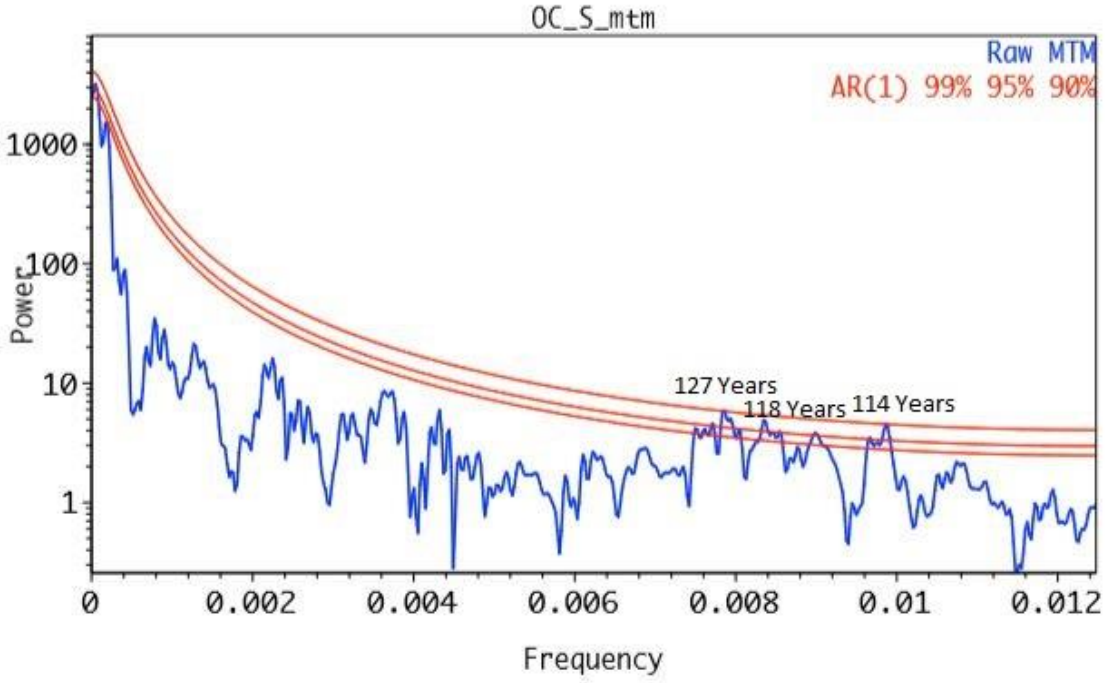

Figure 25 - Organic carbon to sulfur ratio spectral analysis. Periodicity is labelled at 99% and 95% confidence levels. Cycles are observed at 127, 118 and 114 years.

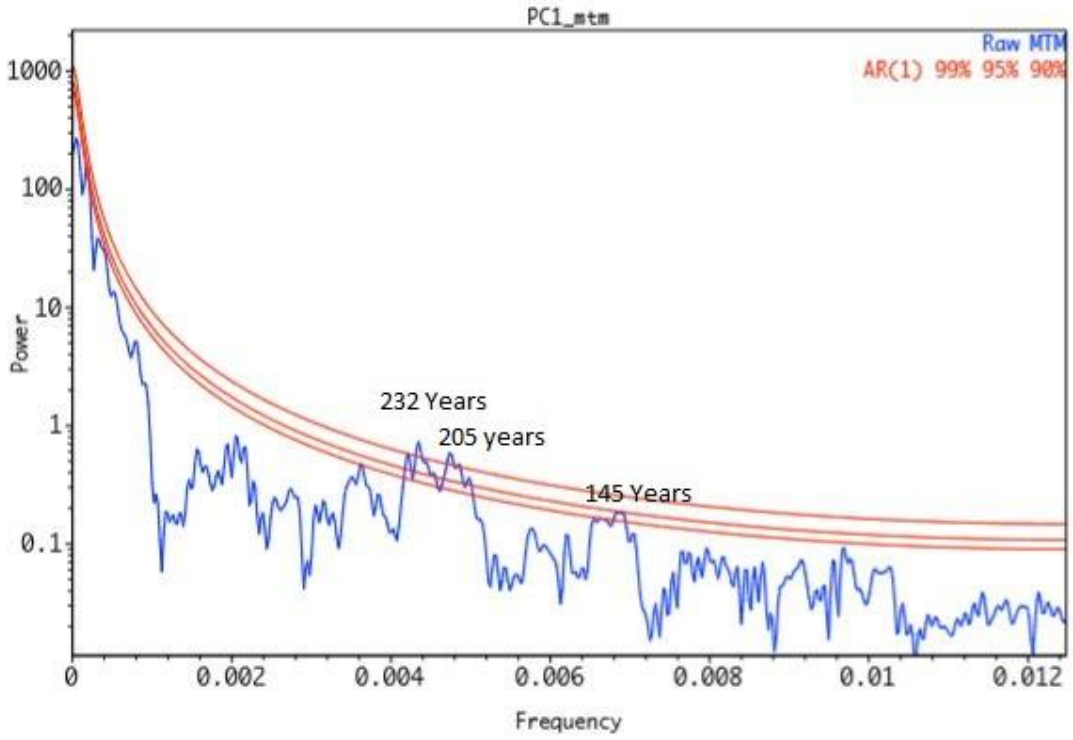

Figure 26 - Principal component 1 spectral analysis. Periodicity is labelled at 99% and 95% confidence levels. Cycles are observed at 232, 205 and 145 years.

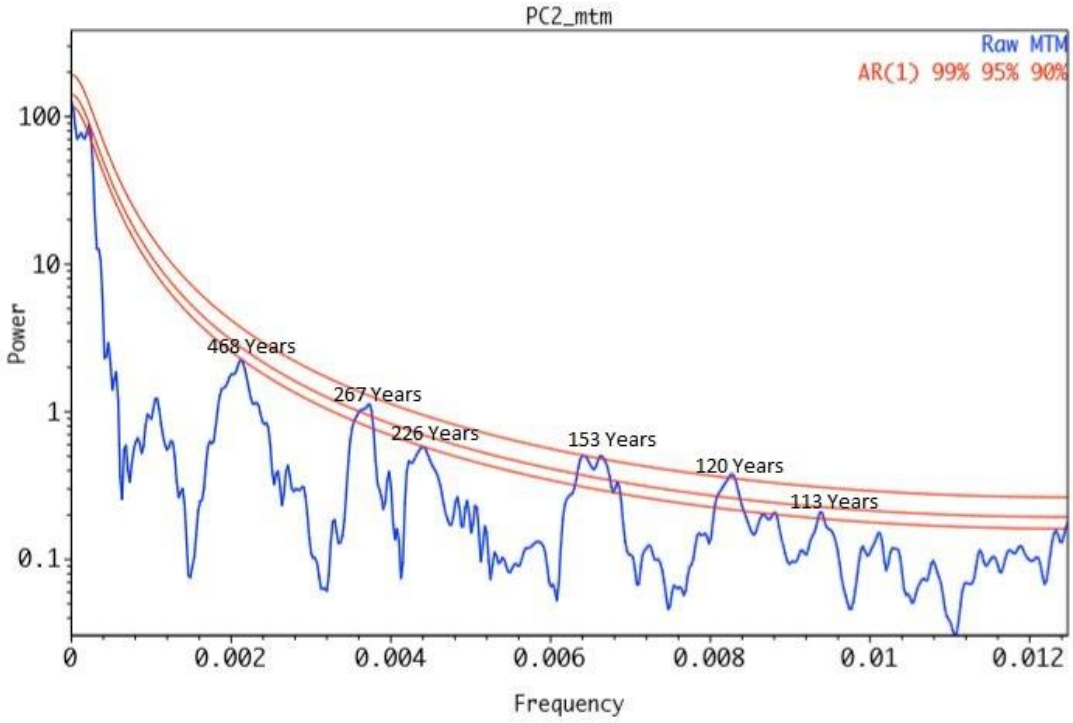

Figure 27- Principal component 2 spectral analysis. Periodicity is labelled at 99%, 95% and 90% confidence levels. Cycles are observed at 468, 267, 226, 153, 120 and 113 years.

7. Tables

	δ13C	δ15N	δ34S	%OC	%N	%S	OC/N	OC/S
δ13C		1.97E-24	4.39E-05	4.99E-25	5.45E-37	5.96E-07	0.000202	1.92E-30
δ15N	0.58583		8.71E-19	3.50E-44	9.53E-41	0.83467	0.27763	3.73E-15
δ34S	-0.2554	-0.53003		2.60E-17	1.16E-10	2.30E-22	2.06E-05	0.049529
%OC	0.58259	0.73758	-0.50126		2.15E-109	0.72349	0.003942	1.21E-32
%N	0.68247	0.71701	-0.393	0.92355		0.031494	0.001635	1.26E-43
%S	-0.30775	0.013458	-0.56365	0.022351	-0.13527		2.34E-10	5.16E-36
OC/N	-0.22856	0.068926	-0.26578	0.17821	-0.1944	0.38487		0.003466
OC/S	0.63907	0.47615	0.12436	0.65702	0.73145	-0.68235	-0.18312	

Table 1 - Correlation matrix. This matrix is based on data starting at 300 cm to base of the core. That is to capture the HCO and YD. The bottom left shows R coefficient values. Orange boxes contain R values with a P value less than 0.01, this shows there is 99% confidence that there is a relationship between two proxies. Blue boxes are R values greater than 0.70 with P values less than 0.01. R values that are close to ±1.00 have the strongest relationships. The upper right indicated P values between proxies. Green boxes have P values less than 0.01 meaning that there is 99% confidence. Yellow boxes have P values between 0.01 and 0.05 which indicate 95% confidence.

PC	Eigenvalue	% variance
1	3.89425	48.678
2	2.20131	27.516
3	0.869999	10.875
4	0.423273	5.2909
5	0.318549	3.9819
6	0.239991	2.9999
7	0.0464223	0.58028
8	0.00620678	0.077585

Table 2 - Summary of Principal Component Analysis showing the eigenvalues of each PC and percentage of variance that each component accounts for.

Proxy	PC 1	PC 2
d13C	0.40611	-0.11114
d15N	0.41588	0.18459
d34S	-0.20871	-0.53234
%OC	0.46155	0.17002
%N	0.48146	0.008977
%S	-0.11707	0.59985
OC/N	-0.04712	0.40468
OC/S	0.39725	-0.34297

Table 3 - PCA loadings for PC1 and PC2. Values highlighted in blue show the proxies with the strongest R value for each PC. PC1 is interpreted as productivity and PC2 is interpreted as oxidation - reduction conditions.

Table 1
Spectral estimates of centennial-scale solar variability

Reference	Record	Spectral method[a]	Detrend method	Length (kyr)	Period (yr)	Period (yr)	Period (yr)	Period (yr)
This work	^{14}C production	MT	First difference	10.0	703	512	352	286
Damon and Peristykh (2000)	$\Delta^{14}C$	Welch	Spline	9.1	706	512	353	288
Stuiver and Braziunas (1989)	$\Delta^{14}C$	ME	Spline	9.6		504	355	299
Damon and Jirikowic (1992)	$\Delta^{14}C$	ME		7.2		526	356	300
Sonett and Finney (1990)	$\Delta^{14}C$	dFt, ME	Polynomial	9.0	717		357	
Periods necessary to model the Hulu Cave spectrum as a heterodyne response					716	501	352	285

[a]MT = multi-taper, ME = maximum entropy, dFt = discrete Fourier transform.

Table 4 - Table taken from S.C. Clemens (2005). This table lays out potential centennial-scale solar variability cycles as hypothesized by multiple sources. This table is used as reference for interpreting solar variability within the data in this research.

Works Cited

Aizenshtat, Z. and Amrani, A., 2004. Significance of δ34S and evaluation of its imprint on sedimentary organic matter: I. The role of reduced sulfur species in the diagenetic stage: A conceptual review. The Geochemical Society Special Publications (Vol. 9, pp. 15-33). Elsevier.

Alley, R.B., Meese, D.A., Shuman, C.A., Gow, A.J., Taylor, K.C., Grootes, P.M., White, J.W.C., Ram, M., Waddington, E.D., Mayewski, P.A. and Zielinski, G.A., 1993. Abrupt increase in Greenland snow accumulation at the end of the Younger Dryas event. Nature, 362(6420), p.527.

Alley, R.B., 2000. The Younger Dryas cold interval as viewed from central Greenland. Quaternary science reviews, 19(1-5), pp.213-226.

Bartlein, P.J., Harrison, S.P., Brewer, S., Connor, S., Davis, B.A.S., Gajewski, K., Guiot, J., Harrison-Prentice, T.I., Henderson, A., Peyron, O. and Prentice, I.C., 2011. Pollen-based continental climate reconstructions at 6 and 21 ka: a global synthesis. Climate Dynamics, 37(3-4), pp.775-802.

Bertrand , S.; Sterken, M.; Vargas-Ramirez, L.; De Batist, M.; Vyverman, W.; Lepoint, G. and Fagel, N.; 2010, Bulk Organic geochemistry of sediments from Puyehue Lake and its watershed (Chile 40°S): Implications for paleoenvironmental reconstructions: Paleoclimatology, Paleoecology, v. 294, p.56-71.

Brauer, A., Endres, C., Günter, C., Litt, T., Stebich, M. and Negendank, J.F., 1999. High resolution sediment and vegetation responses to Younger Dryas climate change in varved lake sediments from Meerfelder Maar, Germany. Quaternary Science Reviews, 18(3), pp.321-329.

Brauer, A., Haug, G.H., Dulski, P., Sigman, D.M. and Negendank, J.F., 2008. An abrupt wind shift in western Europe at the onset of the Younger Dryas cold period. Nature Geoscience, 1(8), p.520.

Broecker, W., Denton, G., Edwards, L., Cheng, H., Alley, R., and Putnam, A., 2010, Putting the Younger Dryas cold event into context: Quaternary Science Reviews, p. 1078-1081.

Clark, P., Dyke, A., Shakun, J., Carlson, A., Clark, J., Wohlfarth, B., Mitrovica, J., Hostetler, S., and McCabe, M., 2009, The Last Glacial Maximum: Science, p. 710-714.

Clemens, S.C., 2005. Millennial-band climate spectrum resolved and linked to centennial-scale solar cycles. Quaternary Science Reviews, 24(5-6), pp.521-531.

Coleman, J., and Friesz, P., 2001, Geohydrology and limnology of Walden Pond, Concord, Massachusetts: USGS, Report 2001-4137, 1-61 p.

Dansgaard, W., 2004. Frozen annals: Greenland ice cap research. Narayana Press.

Davis Jr, R.A., Yale, K.E., Pekala, J.M. and Hamilton, M.V., 2003. Barrier island stratigraphy and Holocene history of west-central Florida. Marine Geology, 200(1-4), pp.103-123.

Dorale, J.A., Wozniak, L.A., Bettis III, E.A., Carpenter, S.J., Mandel, R.D., Hajic, E.R., Lopinot, N.H. and Ray, J.H., 2010. Isotopic evidence for Younger Dryas aridity in the North American midcontinent. Geology, 38(6), pp.519-522

Harris, D., Horwath, W., and van Kessel, C., 2001, Acid fumigation of soils to remove carbonates prior to total organic carbon or CARBON-13 isotopic analysis: Soil Science Society, v. 65, p. 1853-1856.

Huang, Y.; Shuman, B.; Webb III, T.; Grimm, E.C. and Jacobson Jr., G.L.; 2006, Climatic and environmental controls on the variation of C_3 and C_4 plant abundances in central Florida for the past 62,000 years: Paleogeography, Paleoclimatology, Paleoecology, v. 34, no. 7, p. 301-326

Hubeny, J.B., McCarthy, F., M.G, Lewis, J., Drljepan, M., and Morisette, C., 21 January 2015, The paleohydrology of Sluice Pond, NE Massachusetts, and its regional significance: p. 1-16.

Kirby, M., Patterson, W., Mullins, H. and Burnett, A., 2002. Post-Younger Dryas climate interval linked to circumpolar vortex variability: isotopic evidence from Fayetteville Green Lake, New York. Climate Dynamics, 19(3-4), pp.321-330

Knights, C., and Hubeny, J.B., 2016, Paleolimnological Variability of Multiple Lake Basins in Walden Pond, MA. p. 9-10.

Koteff, C., 1964, Surficial geology of the Concord quadrangle, Massachusetts: USGS, Report GQ-331.

Likens, G.E., and Davis, M.B., 1975, Post-Glacial History of Mirror Lake and Its Watershed In New Hampshire, U. S. A.: An Initial Report: Verhandlungen Internationale Vereinigung Limnologie, v. 19, p. 982-993.

Mangerud, J.A.N., Andersen, S.T., Berglund, B.E. and Donner, J.J., 1974. Quaternary stratigraphy of Norden, a proposal for terminology and classification. Boreas, 3(3), pp.109-126.

Matero, I.S.O., Gregoire, L.J., Ivanovic, R.F., Tindall, J.C. and Haywood, A.M., 2017. The 8.2 ka cooling event caused by Laurentide ice saddle collapse. Earth and Planetary Science Letters, 473, pp.205-214.

Meyers, P.A., and Ishiwatari, R.; 1993. Lacustrine organic geochemistry ---an overview of indicators of organic matter sources and diagenesis in lake sediments: Organic Geochemistry, v. 20, p. 867-900.

Meyers, P.A., and Lallier - Verges, E; 1999, Lacustrine sedimentary organic matter records of Late Quaternary paleoclimates: Journal of Paleolimnology, v. 21, p.345-372.
Meyers, P. A., and Teranes, L.J., 1997, Sediment Organic Matter: Tracking Environmental Change using Lake Sediments, v. Volume 2, p. 239-270.

Rasmussen, S.O., Andersen, K.K., Svensson, A.M., Steffensen, J.P., Vinther, B.M., Clausen, H.B., Siggaard-Andersen, M.L., Johnsen, S.J., Larsen, L.B., Dahl-Jensen, D. and Bigler, M., 2006. A new Greenland ice core chronology for the last glacial termination. Journal of Geophysical Research: Atmospheres, 111(D6)

Rudd, J.W., Kelly, C.A. and Furutani, A., 1986. The role of sulfate reduction in long term accumulation of organic and inorganic sulfur in lake sediments. Limnology and oceanography, 31(6), pp.1281-1291.

Ruddiman, W., 2014, Warmer, The Cooler North Polar Summers, in Earth's Climate: Past and Future: New York, W.H. Freeman and Company, p. 288-290.

Stager, K., Wiltse, B., Hubeny, J.B., Yankowsky, E., Nardelli, D., and Primack, R., 2018, Climate variability and cultural eutrophication at Walden Pond (Massachusetts, USA) during the last 1800 years: PLOS One, p. 1-21.

Thomas, E.R., Wolff, E.W., Mulvaney, R., Steffensen, J.P., Johnsen, S.J., Arrowsmith, C., White, J.W., Vaughn, B. and Popp, T., 2007. The 8.2 ka event from Greenland ice cores. Quaternary Science Reviews, 26(1-2), pp.70-81.

.

.